

Article

Carboxylate-Assisted #-(*Z*) Stereoselective Hydrosilylation of Terminal Alkynes Catalyzed by a Zwitterionic Bis-NHC Rhodium(III) Complex

Raquel Puerta-Oteo, Julen Munarriz, Victor Polo, M. Victoria Jiménez, and Jesús J. Pérez-Torrente

ACS Catal., Just Accepted Manuscript • DOI: 10.1021/acscatal.0c01582 • Publication Date (Web): 05 Jun 2020

Downloaded from pubs.acs.org on June 5, 2020

Just Accepted

“Just Accepted” manuscripts have been peer-reviewed and accepted for publication. They are posted online prior to technical editing, formatting for publication and author proofing. The American Chemical Society provides “Just Accepted” as a service to the research community to expedite the dissemination of scientific material as soon as possible after acceptance. “Just Accepted” manuscripts appear in full in PDF format accompanied by an HTML abstract. “Just Accepted” manuscripts have been fully peer reviewed, but should not be considered the official version of record. They are citable by the Digital Object Identifier (DOI®). “Just Accepted” is an optional service offered to authors. Therefore, the “Just Accepted” Web site may not include all articles that will be published in the journal. After a manuscript is technically edited and formatted, it will be removed from the “Just Accepted” Web site and published as an ASAP article. Note that technical editing may introduce minor changes to the manuscript text and/or graphics which could affect content, and all legal disclaimers and ethical guidelines that apply to the journal pertain. ACS cannot be held responsible for errors or consequences arising from the use of information contained in these “Just Accepted” manuscripts.

1
2
3
4
5
6
7
8
9
10
11
12
13
14
15
16
17
18
19
20
21
22
23
24
25
26
27
28
29
30
31
32
33
34
35
36
37
38
39
40
41
42
43
44
45
46
47
48
49
50
51
52
53
54
55
56
57
58
59
60

Carboxylate-Assisted β -(Z) Stereoselective Hydrosilylation of Terminal Alkynes Catalyzed by a Zwitterionic Bis-NHC Rhodium(III) Complex.

Raquel Puerta-Oteo,^a Julen Munarriz,^{b,c} Víctor Polo,^b M. Victoria Jiménez,^{a,} and Jesús J. Pérez-Torrente.^{a,*}*

(a) Departamento de Química Inorgánica, Instituto de Síntesis Química y Catálisis Homogénea (ISQCH), Universidad de Zaragoza–CSIC, Facultad de Ciencias, C/ Pedro Cerbuna 12, 50009 Zaragoza, Spain.

(b) Departamento de Química Física, Instituto de Biocomputación y Física de Sistemas Complejos (BIFI), Universidad de Zaragoza, Facultad de Ciencias, C/ Pedro Cerbuna 12, 50009 Zaragoza, Spain.

(c) Department of Chemistry & Biochemistry, University of California Los Angeles (UCLA), Los Angeles, California 90095, United States.

KEYWORDS: Hydrosilylation, Alkynes, Vinylsilanes, Rhodium, N-heterocyclic carbenes

1
2
3
4
5
6
7
8
9
10
11
12
13
14
15
16
17
18
19
20
21
22
23
24
25
26
27
28
29
30
31
32
33
34
35
36
37
38
39
40
41
42
43
44
45
46
47
48
49
50
51
52
53
54
55
56
57
58
59
60

ABSTRACT

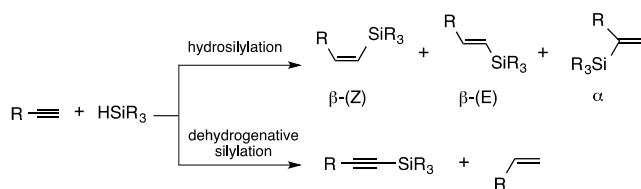
The zwitterionic compound $[\text{Cp}^*\text{RhCl}\{(\text{MeIm})_2\text{CHCOO}\}]$ is an efficient catalyst for the hydrosilylation of terminal alkynes with excellent regio- and stereoselectivity towards the less thermodynamically stable β -(*Z*)-vinylsilane isomer under mild reaction conditions. A broad range of linear 1-alkynes, cycloalkyl acetylenes and aromatic alkynes undergo the hydrosilylation with HSiMe_2Ph to afford the corresponding β -(*Z*)-vinylsilanes in quantitative yields in short reaction times. The reaction of aliphatic alkynes with HSiEt_3 is slower, resulting in a slight decrease of selectivity towards the β -(*Z*)-vinylsilane product, which is still greater than 90%. However, a significant selectivity decrease is observed in the hydrosilylation of aromatic alkynes due to the β -(*Z*) \rightarrow β -(*E*) vinylsilane isomerization. Moreover, the hydrosilylation of bulky alkynes, such as *t*-Bu-C \equiv CH or Et₃SiC \equiv CH, is unselective. Experimental evidences suggest that the carboxylate function plays a key role in the reaction mechanism, which has been validated by means of DFT calculations, as well as by mass spectrometry and labelling studies. On the basis of previous results, we propose an ionic outer-sphere mechanism pathway in which the carboxylate fragment acts as a silyl carrier. Namely, the hydrosilylation mechanism entails the heterolytic activation of the hydrosilane assisted by the carboxylate function to give the hydrido intermediate $[\text{Cp}^*\text{RhH}\{(\text{MeIm})_2\text{CHCOO-SiR}_3\}]^+$. The transference of the silylium moiety from the carboxylate to the alkyne results in the formation of a flat β -silyl carbocation intermediate that undergoes a hydride transfer from the Rh(III) center to generate the vinylsilane product. The outstanding β -(*Z*) selectivity results from the minimization of the steric interaction between the silyl moiety and the ligand system in the hydride transfer transition state.

INTRODUCTION

Vinylsilanes are valuable building blocks in organic synthesis, polymer chemistry and materials science because of their versatility, ease of handling, low toxicity, and reasonable stability relative to other vinyl-metal species.¹ They have been traditionally prepared by stoichiometric methods from organometallic reagents and the development of more sustainable synthetic strategies for their production is still an important current scientific challenge.

Transition-metal-catalyzed hydrosilylation of alkynes has been regarded as one of the most straightforward and atom-economical methodologies for accessing versatile vinylsilanes. However, the hydrosilylation of terminal alkynes can afford several vinylsilanes isomers and thus, the control of the regio- and stereoselectivity along the H–Si addition process is a major issue (see Scheme 1).² The Markovnikov addition results in the formation of the α -vinylsilane isomer. However, the reaction may as well proceed with anti-Markovnikov regioselectivity to afford the β -(*E*)-vinylsilane and β -(*Z*)-vinylsilane stereoisomers, the syn- and anti-addition reaction products, respectively. The selective synthesis of α - and β -(*Z*)-vinylsilanes is considered to be more challenging than the formation of the thermodynamically more stable β -(*E*)-vinylsilane isomer.^{2d} In this context, the β -(*Z*) isomerization to β -(*E*)-vinylsilanes under reaction conditions is an additional hurdle to the development of the β -(*Z*)-selective alkyne hydrosilylation catalysts. Furthermore, the formation of the competitive dehydrogenative silylation products, namely alkynylsilane and the corresponding alkene, has been frequently observed for some catalysts (Scheme 1).³ Even though a number transition-metal-based catalysts including both noble-metals, such as Rh,⁴ Ir⁵ and Ru,⁶ and more recently base-metals, such as Co, Fe⁷ and Mn,⁸ for the preparation of β -(*Z*)-vinylsilanes have been reported, the development of improved catalysts to overcome the thermodynamic stability of the β -(*E*)-vinylsilane with wider applicability is still necessary. In this context, a deeper understanding of the reaction mechanisms is pivotal for the rational design of more active and selective catalytic systems.

1
2
3 The catalytic hydrosilylation of terminal alkynes usually proceeds with anti-Markovnikov
4 regiochemistry and predominantly syn-addition stereochemistry, which can be rationalized by
5 the classic inner-sphere Chalk-Harrod mechanism. This mechanism has been put forward to
6 explain the formation of the β -(*E*)-vinylsilane isomer in Pt-based transition-metal catalysts.⁹
7
8 However, it cannot account for the formation of the β -(*Z*)-vinylsilane isomer or the
9 alkyne-silane product resulting from the dehydrogenative silylation process. The formation of
10 both types of products can be explained by a modified Chalk-Harrod mechanism that entails
11 the silylmetalation of the alkyne by migratory insertion into the M-Si bond, instead the M-H
12 bond, to give a (*Z*)-silylvinylene metal complex.¹⁰ The formation of the β -(*Z*)-vinylsilane
13 requires the metal-assisted isomerization of the (*Z*)-silylvinylene to the thermodynamically
14 more favorable (*E*)-silylvinylene through the well-established Crabtree¹¹ and Ojima¹²
15 mechanisms, which involve a metallacyclopropene or zwitterionic carbene species,
16 respectively. However, the metal-catalyzed hydrosilylation reactions can also proceed through
17 a heterolytic Si-H bond cleavage that gives rise to silylium-type putative catalytic
18 intermediates.¹³ This mode of activation of silanes constitutes an important alternative to the
19 conventional Chalk-Harrod mechanism that entails the oxidative addition of the silane Si-H
20 bond at the metal center. Such advances have paved the way for the rational design of more
21 active and selective catalysts.¹⁴
22
23
24
25
26
27
28
29
30
31
32
33
34
35
36
37
38
39
40
41
42
43



53 **Scheme 1.** Hydrosilylation and dehydrogenative silylation of terminal alkynes.
54
55

56
57 Importantly, ligand design plays a crucial role when proposing novel catalysts, as they are
58 able to modulate the steric and electronic properties of the metal center. In this sense, N-
59
60

1
2
3 heterocyclic carbenes (NHCs) have become ubiquitous as ligands in transition metal mediated
4
5 homogeneous catalysis due the easy access to a variety of topologies with tuned electronic
6
7 properties that adapt to the specific requirements of individual catalytic transformations.¹⁵ In
8
9 this context, there has been a significant interest in the development of alkyne hydrosilylation
10
11 rhodium catalysts based on functionalized N-heterocyclic carbene ligands of hemilabile
12
13 character.¹⁶ Recently, we have proposed a novel ionic outer-sphere mechanism for the
14
15 hydrosilylation of terminal alkynes catalyzed by $[M^{III}(\text{bis-NHC})_2]^+$ ($M = \text{Ir, Rh}$; bis-NHC =
16
17 methylene-bis(N-2-methoxyethyl)imidazole-2-ylidene) complexes, featuring a bis-NHC ligand
18
19 functionalized with labile 2-methoxyethyl groups at the wingtips, able to explain the selective
20
21 formation of the β -(Z)-vinylsilane isomer.¹⁷ This outer-sphere mechanism involves the
22
23 heterolytic splitting of the hydrosilane assisted by the metal center and a molecule of acetone,
24
25 which is the reaction solvent, that acts as a silane-shuttle and transfers the silylium moiety to
26
27 the alkyne. In sharp contrast, the related rhodium complex $[\text{Rh}^{III}(\text{bis-NHC})(\text{CF}_3\text{COO})_2]^+$ is
28
29 selective for the α -vinylsilane isomer in the hydrosilylation of a wide range of terminal alkynes
30
31 which is believed to proceed with the assistance of the trifluoroacetate ligands.¹⁸ These results
32
33 point out the wide variability in the catalytic selectivity when tuning the non-innocent ligands,
34
35 as a consequence of their active participation in the catalytic steps.
36
37
38
39
40
41

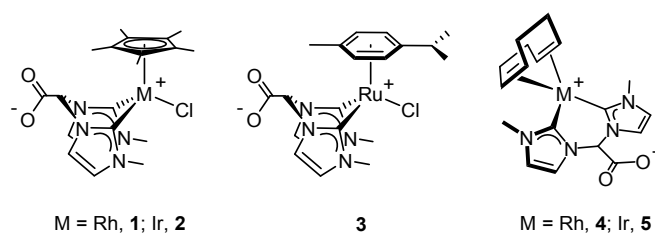
42
43 Our group has an ongoing research interest on the potential of a carboxylate-functionalized
44
45 methylene-bridged bis-NHC ligand for the construction of a versatile metal-ligand platform
46
47 with application in catalysis.¹⁹ In this regard, we have shown that zwitterionic iridium
48
49 complexes such as $[\text{Ir}(\text{cod})\{(\text{MeIm})_2\text{CHCOO}\}]$ and $[\text{Cp}^*\text{IrCl}\{(\text{MeIm})_2\text{CHCOO}\}]$ ($\text{MeIm} = 3$ -
50
51 methylimidazol-2-yliden-1-yl) efficiently catalyze both the hydrogenation of CO_2 to formate,²⁰
52
53 and the oxidation of water using chemical oxidants.²¹ In both cases, experimental and theoretical
54
55 studies have shown that the κ^3 -C,C',O-tridentate coordination mode of the functionalized bis-
56
57 NHC ligand plays a key role in the stabilization of catalytic intermediates. However, the
58
59 carboxylate function at the linker not only confers hemilabile properties to the ligand but also
60

1
2
3 behaves as a reactive site. In this sense, we have shown that the carboxylate moiety in
4
5 [Cp*IrCl{(MeIm)₂CHCOO}] is involved in the precatalyst activation step leading to the active
6
7 species for the reduction of CO₂ with hydrosilanes to silylformates.²²
8
9

10 These precedents and the potential of the uncoordinated carboxylate moiety to assist non-
11
12 classical hydrosilylation pathways such as a silane-shuttle or proton-shuttle, facilitating the
13
14 alkyne-vinylidene tautomerization,²³ have prompted us to study the catalytic activity of the
15
16 related rhodium(III) compound [Cp*RhCl{(MeIm)₂CHCOO}] in the hydrosilylation of
17
18 terminal alkynes. Remarkably, the investigation of the reaction mechanism has disclosed the
19
20 key role of the carboxylate fragment in the selective formation of the less thermodynamically
21
22 stable β-(Z) isomer in the hydrosilylation of terminal alkynes. This catalyst constitutes a step
23
24 forward in the exploration of new catalysts with unconventional mechanisms.
25
26
27
28
29

30 RESULTS AND DISCUSSION

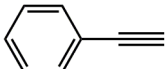
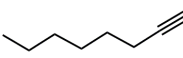
31
32 **Preliminary catalyst screening for terminal alkyne hydrosilylation.** The zwitterionic
33
34 complexes depicted in Chart 1 were screened as catalyst precursors for the hydrosilylation of
35
36 terminal alkynes. The hydrosilylation tests were carried out by using phenylacetylene and oct-
37
38 1-yne as terminal alkynes and dimethylphenylsilane as a representative hydrosilane. The
39
40 catalytic reactions were performed under an argon atmosphere in CDCl₃ at 333 K with 1 mol%
41
42 catalyst loading, [catalyst] = 1.54 mM, and routinely monitored by ¹H NMR spectroscopy with
43
44 anisole as internal standard. The outcome of these preliminary experiments is summarized in
45
46
47
48 Table 1.
49
50
51



1
2
3 **Chart 1.** Selected zwitterionic rhodium, iridium and ruthenium catalyst precursors for
4
5
6
7 terminal alkyne hydrosilylation.
8
9

10
11 The hydrosilylation of phenylacetylene with HSiMe₂Ph catalyzed by the zwitterionic
12 compound [Cp*RhCl{(MeIm)₂CHCOO}] (**1**) was completed in 24 min with full selectivity for
13 the β-(Z)-vinylsilane derivative (entry 1). In sharp contrast, the related iridium(III)-based
14 species, [Cp*IrCl{(MeIm)₂CHCOO}] (**2**), is almost completely inactive and only provides a
15 2% conversion in 24 h (entry 2). The ruthenium(II)-based complex [(*p*-
16 cymene)RuCl{(MeIm)₂CHCOO}] (**3**) is moderately active, with a 71% conversion in 48 h.
17 Nonetheless, it lacks selectivity, affording up to 15% of the undesired alkene by-product, which
18 results from the dehydrogenative silylation of the alkyne (entry 3). Along the rhodium(I) and
19 iridium(I) series, the rhodium complex [Rh(cod){(MeIm)₂CHCOO}] (**4**) was found to be active
20 in the polymerization of phenylacetylene (PA) producing polyphenylacetylene (PPA) in the
21 early stage of the reaction even when the order of addition of the reagents was reversed
22 (HSiMe₂Ph before than PA). The PPA was identified in the ¹H NMR spectra of the reaction
23 mixture due to its characteristic set of resonances at δ 6.9, 6.6 and 5.8 (=CH) ppm.²⁴ In the case
24 of catalyst precursor **4** the selectivity in PPA was 63% after 1 hour (35% conversion) and 18%
25 after 24 h (98% conversion) (entries 4 and 5). The iridium-based complex
26 [Ir(cod){(MeIm)₂CHCOO}] (**5**) does not show activity in polymerization and affords a 95% of
27 conversion in 24 h. However, it is unselective, providing a 30% of the alkene by-product, as
28 well as similar proportions of the β-(Z), β-(E), and α-vinylsilane derivatives (entry 6). The
29 performance of the catalyst precursors in the hydrosilylation of oct-1-yne follows a similar trend
30 as that observed for phenylacetylene. Noteworthy, catalyst [Cp*RhCl{(MeIm)₂CHCOO}] (**1**)
31 is by far the most active and selective one, enabling full conversion to β-(Z)-vinylsilane in 24
32 min (entry 7).
33
34
35
36
37
38
39
40
41
42
43
44
45
46
47
48
49
50
51
52
53
54
55
56
57
58
59
60

Table 1. Hydrosilylation of terminal alkynes with HSiMe₂Ph catalyzed by zwitterionic carboxylate bridge-functionalized bis-NHC rhodium, iridium and ruthenium complexes.^{a,b}

entry	alkyne	catalyst	time (h)	conv. (%)	β-(Z) (%)	β-(E) (%)	α (%)	alkene (%)
1		1	0.4	>99	>99	---	---	---
2		2	24	2	50	50	---	---
3		3	48	71	46	29	10	15
4		4	1	35 ^c	13	15	8	---
5		4	24	98 ^c	---	74	8	---
6		5	24	95	32	24	14	30
7		1	0.4	>99	>99	---	---	---
8		2	24	1	85	15	---	---
9		4	24	88	95	3	---	2
10		5	24	91	18	26	29	27

a) Experiments were carried out in CDCl₃ at 333 K using a HSiMe₂Ph/RC≡CH/catalyst ratio of 100/100/1, [catalyst] = 1.54 mM. b) Conversion and selectivities determined by ¹H NMR using anisole as internal standard. c) HSiMe₂Ph was added before phenylacetylene. Selectivity towards PPA = 63% after 1 h and 18% after 24h.

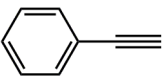
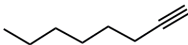
Remarkably, catalyst precursor **1** is highly soluble in water owing to the presence of an uncoordinated carboxylate function at the bis-NHC ligand. In this regard, we envisaged it as a potential pre-catalyst for the hydrosilylation in water, and thus performed an in-depth investigation of such process. In this context, it is worth mentioning that highly efficient and stereoselective water-soluble catalysts for the hydrosilylation of terminal alkynes based on platinum²⁵ and copper²⁶ have recently been reported, paving the way to the development of a new generation of clean and sustainable catalysts. Unfortunately, **1** exhibited a poor catalytic

1
2
3 activity in the hydrosilylation of oct-1-yne with HSiMe₂Ph in water even when using the phase
4 transfer agent TEBA (triethylbenzylammonium chloride). Namely, only a 14% alkyne
5 conversion was attained after 24h at 333 K with 46% selectivity for the β -(*E*)-vinylsilane.
6
7 However, the ¹H NMR of the yellow oil extracted showed the presence of unreacted alkyne,
8 but no hydrosilane which suggests that compound **1** could also catalyze the hydrolysis of the
9 hydrosilane.²⁷ In fact, in an independent experiment, we have found that **1** catalyzes the
10 hydrolysis of HSiMe₂Ph, which confirms that this process competes with the alkyne
11 hydrosilylation (see Experimental Section for additional details).
12
13
14
15
16
17
18
19
20

21 **Hydrosilylation of 1-alkynes catalyzed by 1: influence of the temperature and catalyst**
22 **loading.** The outstanding catalytic performance exhibited by [Cp**Rh*Cl{(MeIm)₂CHCOO} (**1**)
23 prompted us to study the influence of the temperature and catalyst loading in the catalytic
24 activity and selectivity. Therefore, in order to compare with the results obtained at 333 K, the
25 hydrosilylation reactions were also performed at room temperature (RT). So as to better
26 understand the catalyst behavior, two hydrosilanes, HSiMe₂Ph and HSiEt₃, and two substrates,
27 phenylacetylene and oct-1-yne, were selected. In addition, the influence of the catalyst loading
28 was studied. For that, several experiments decreasing the catalyst loading from 1 to 0.1 mol%
29 (HSiR₃/RC≡CH/catalyst ratio of 1000/1000/1) were carried out. The results are summarized in
30 Table 2.
31
32
33
34
35
36
37
38
39
40
41
42
43

44 As expected, the hydrosilylation of phenylacetylene and oct-1-yne was slower at RT than at
45 333 K, especially in the case of HSiEt₃. For example, full conversion in the hydrosilylation of
46 oct-1-yne with HSiMe₂Ph and HSiEt₃ requires 7 and 48 h at RT, respectively (entries 10 and
47 14) vs. 0.4 and 6 h at 333 K (entries 9 and 13). Interestingly, in both cases the excellent regio-
48 and stereoselectivity for the β -(*Z*)-vinylsilane isomer is maintained at RT. The same trend was
49 observed in the hydrosilylation of phenylacetylene. Remarkably, an improvement of the β -(*Z*)
50 selectivity up to 98% was attained in the hydrosilylation of phenylacetylene at RT using HSiEt₃
51 as hydrosilane (entry 6).
52
53
54
55
56
57
58
59
60

Table 2. Influence of the temperature and catalyst loading in the hydrosilylation of terminal alkynes catalyzed by $[\text{Cp}^*\text{RhCl}\{(\text{Melm})_2\text{CHCOO}\}]$ (**1**).^{a,b}

entry	alkyne	hydrosilane	T (K)	t (h)	conv. (%)	S/C ratio	Selectivity (%)
							β -(Z)/ β -(E)/ α /alkene
1		HSiMe ₂ Ph	333	0.4	>99	100	>99 / - / - / -
2		HSiMe ₂ Ph	RT	5	99	100	>99 / - / - / -
3		HSiMe ₂ Ph	333	48	100	1000	78 / 18 / 3 / 1
4		HSiMe ₂ Ph	RT	48	100	1000	>99 / - / - / -
5		HSiEt ₃	333	9.5	91	100	83 / 10 / 4 / 3
6		HSiEt ₃	RT	48	49	100	98 / 1 / 1 / -
7		HSiEt ₃	333	72	43	1000	58 / 42 / - / -
8		HSiEt ₃	RT	120	7	1000	86 / 12 / 1 / 1
9		HSiMe ₂ Ph	333	0.4	>99	100	>99 / - / - / -
10		HSiMe ₂ Ph	RT	7	97	100	>99 / - / - / -
11		HSiMe ₂ Ph	333	48	82	1000	89 / 7 / 3 / 1
12		HSiMe ₂ Ph	RT	48	75	1000	95 / 4 / - / 1
13		HSiEt ₃	333	6	93	100	94 / - / - / 6
14		HSiEt ₃	RT	48	100	100	96 / - / - / 4
15		HSiEt ₃	333	96	98	1000	97 / - / - / 3
16		HSiEt ₃	RT	24	3	1000	>99 / - / - / -

a) Experiments were carried out in CDCl₃ using a HSiR₃/RC≡CH ratio of 1/1, [1] = 1.54 mM, S/C = substrates/catalyst ratio. b) Conversion and selectivities determined by ¹H NMR using anisole as internal standard.

When the catalyst loading is reduced up to 0.1 mol%, longer reaction times are needed to achieve acceptable conversion levels. In accord with the results described in the previous

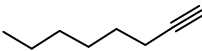
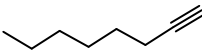
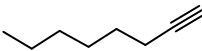
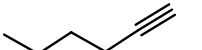
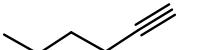
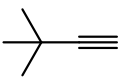
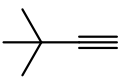
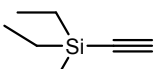
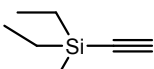
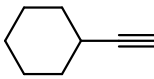
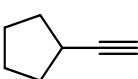
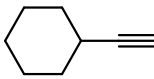
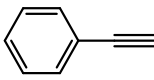
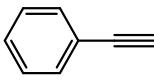
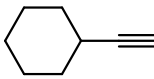
1
2
3 section, HSiEt₃ is the hydrosilane that shows lowest reaction rates. Under these reaction
4 conditions, the catalytic activity in the hydrosilylation of both phenylacetylene and oct-1-yne
5 with HSiEt₃ at RT was very low (entries 8 and 16) although increased appreciably at 333 K
6 (entries 7 and 15). However, the long reaction times at this temperature are at the expense of a
7 significant decrease in the selectivity in the case of the hydrosilylation of phenylacetylene. This
8 is likely to be a consequence of the β -(Z)→ β -(E) vinylsilane isomerization (entry 7).
9
10 Interestingly, 98% conversion in 96 h was attained in the hydrosilylation of oct-1-yne with a
11 97% of selectivity in β -(Z)-vinylsilane (entry 15).
12
13
14
15
16
17
18
19
20
21

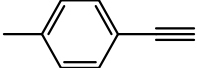
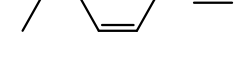
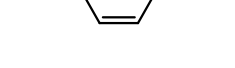
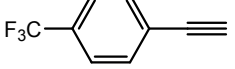
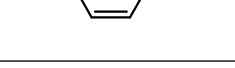
22 Remarkably, the hydrosilylation of phenylacetylene and oct-1-yne with HSiMe₂Ph at 333 K
23 with 0.1 mol% catalyst loading resulted in a selectivity decrease (entries 3 and 11). Thus,
24 although conversions higher than 80% were attained in 48 h, the selectivity for β -(Z)-vinylsilane
25 dropped from 99% to 78% and 89% (entries 3 and 11) presumably due to β -(Z)→ β -(E)
26 vinylsilane isomerization. Noteworthy, the hydrosilylation of phenylacetylene with HSiMe₂Ph
27 at RT using 0.1 mol% catalyst loading was completed in 48 h with full selectivity for β -(Z)-
28 vinylsilane (entry 4). Under the same reaction conditions, the hydrosilylation of oct-1-yne
29 yielded a 75% conversion with a selectivity for β -(Z)-vinylsilane as high as 95% (entry 12).
30
31
32
33
34
35
36
37
38
39

40 To our delight, the catalytic performance of **1** is well preserved after several consecutive
41 cycles. The **1**-catalyzed (1 mol%) hydrosilylation of phenylacetylene with HSiMe₂Ph resulted
42 in full conversion in less than half an hour at 333 K (entry 1). The further addition of reactants
43 (phenylacetylene and HSiMe₂Ph) after the reaction completion also led to the steady
44 consumption of the reactants in the same reaction time. The monitoring of the reaction by ¹H
45 NMR evidenced that at the end of the six consecutive reaction experiments, the
46 β -(Z)-vinylsilane isomer was the only obtained product (see Supporting Information for more
47 details). Thus, catalyst precursor **1** was able to perform at least six consecutive catalytic cycles
48 without losing neither activity nor selectivity towards the β -(Z)-vinylsilane isomer, pointing
49 out the outstanding selectivity induced by **1**.
50
51
52
53
54
55
56
57
58
59
60

Hydrosilylation of 1-alkynes catalyzed by 1: substrate scope. Catalyst precursor $[\text{Cp}^*\text{RhCl}\{(\text{MeIm})_2\text{CHCOO}\}]$ (**1**) allows for the hydrosilylation of a range of aliphatic and aromatic 1-alkynes using both HSiMe_2Ph and HSiEt_3 . As can be seen in Table 3, excellent selectivities for the β -(*Z*)-vinylsilane product were obtained at relatively short reaction times when using HSiMe_2Ph as hydrosilane. The reactions with HSiEt_3 required longer reaction times to achieve reasonable conversion values which resulted, in some cases, in a loss of selectivity towards the β -(*Z*)-vinylsilane product.

Table 3. Hydrosilylation of terminal alkynes with HSiMe_2Ph and HSiEt_3 catalyzed by $[\text{Cp}^*\text{RhCl}\{(\text{MeIm})_2\text{CHCOO}\}]$ (**1**).^{a,b}

entry	alkyne	silane	time (h)	conv. (%)	β -(<i>Z</i>) (%)	β -(<i>E</i>) (%)	α (%)	alkene (%)
1		HSiMe_2Ph	0.4	>99	>99	---	---	---
2		HSiMePh_2	1.5	95	>99	---	---	---
3		HSiEt_3	6	98	97	---	---	3
4		HSiMe_2Ph	0.75	100	>99	---	---	---
5		HSiEt_3	18	98	91	3	4	2
6		HSiMe_2Ph	24	91	34	39	19	8
7		HSiEt_3	24	78	13	33	21	33
8		HSiMe_2Ph	24	>99	71	28	---	1
9		HSiEt_3	48	76	29	70	---	1
10		HSiMe_2Ph	3	>99	>99	---	---	---
11		HSiMe_2Ph	3	82	>99	---	---	---
12		HSiMe_2Ph	0.4	>99	>99	---	---	---
13		HSiMePh_2	1.5	95	>99	---	---	---
14		HSiEt_3	9.5	91	83	10	4	3
15		HSiMe_2Ph	0.54	>99	>99	---	---	---

16		HSiEt ₃	4	87	69	28	1	2
17		HSiMe ₂ Ph	1.1	>99	98	2	---	---
18		HSiEt ₃	4	61	51	46	1	2
19		HSiMe ₂ Ph	0.3	>99	94	6	---	---
20		HSiEt ₃	4	87	19	81	---	---
21		HSiMe ₂ Ph	1.7	98	99	---	1	---
22		HSiEt ₃	24	55	90	3	3	4

a) Experiments were carried out in CDCl₃ at 333 K using a HSiR₃/RC≡CH/catalyst ratio of 100/100/1, [1] = 1.54 mM. b) Conversion and selectivities determined by ¹H NMR using anisole as internal standard.

The hydrosilylation of oct-1-yne and hex-1-yne with HSiMe₂Ph was completed in less than one hour and provided >99% selectivity to β-(Z)-vinylsilane (entries 1 and 4). The hydrosilylation of oct-1-yne with the bulkier hydrosilane HSiMePh₂ is slightly slower, also yielding complete selectivity to β-(Z)-vinylsilane (entry 2). Interestingly, an excellent selectivity for the β-(Z)-vinylsilane product was also attained with HSiEt₃ (entries 3 and 5). However, the hydrosilylation of the bulky *t*-Bu-C≡CH with HSiMe₂Ph and HSiEt₃ was completely unselective and gave significant amounts of all the vinylsilane isomers (entries 6 and 7). In sharp contrast, the hydrosilylation of Et₃SiC≡CH was completed in 24 h with an acceptable selectivity towards the β-(Z)-vinylsilane, up to 71% (entry 8). Remarkably, a reverse selectivity towards the β-(E)-vinylsilane was observed with HSiEt₃ giving a 70% selectivity in 48 h (entry 9). Cycloalkyl acetylenes were also efficiently reduced using HSiMe₂Ph. Thus, the hydrosilylation of cyclohexylacetylene and cyclopentylacetylene gave complete selectivity to the β-(Z)-vinylsilane product with conversion values up to >99 and 82%, respectively, in 3 h (entries 10 and 11).

The hydrosilylation of phenylacetylene with HSiMe₂Ph showed the best catalytic performance, with full conversion and selectivity towards the β-(Z)-vinylsilane in 0.4 h (entry

12). Also, a 95% conversion in 1.5 h with complete selectivity to β -(*Z*)-vinylsilane was attained with the bulkier hydrosilane HSiMePh₂ (entry 13). The influence of electronic effects on the hydrosilylation of terminal alkynes was studied in a series of phenylacetylene derivatives with different substituents at the *para* position, 4-R-C₆H₄-C≡CH (R = -CH₃, -*t*Bu, -OCH₃, -CF₃). As can be observed in the selected reaction profiles of Figure 1, the presence of a -OMe electron-donating substituent at the *para* position resulted in an increase in the catalytic activity compared to phenylacetylene. Thus, the hydrosilylation of (4-methoxyphenyl)acetylene with HSiMe₂Ph gave complete conversion in 0.3 h with 94% selectivity towards the β -(*Z*)-vinylsilane (entry 19). In contrast, the hydrosilylation of the phenylacetylene derivative with a -CF₃ electron-withdrawing substituent at the *para* position is much slower, providing a 98% of conversion in 1.7 h (entry 21).

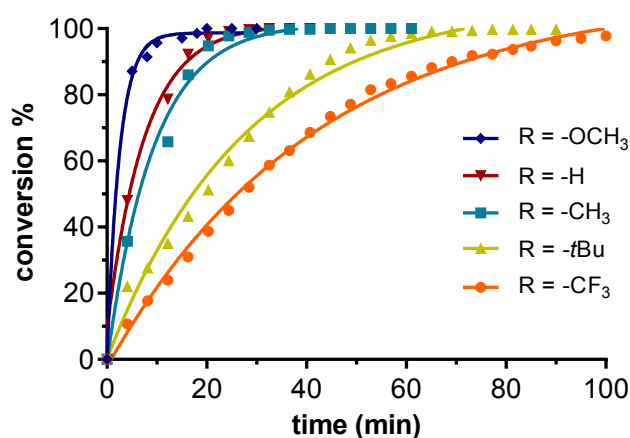


Figure 1. Reaction profile of conversion vs. time for the hydrosilylation of phenylacetylene derivatives 4-R-C₆H₄-C≡CH with HSiMe₂Ph, catalyzed by **1** in CDCl₃ at 333 K.

In general, the presence of weakly electron-donating groups at the *para* position resulted in a decrease of the catalytic activity compared to phenylacetylene (Figure 1). In this sense, although the hydrosilylation of (4-methylphenyl)acetylene with HSiMe₂Ph showed a very similar profile to that of phenylacetylene, the hydrosilylation of (4-*tert*-butylphenyl)acetylene

1
2
3 is much slower and only provides a 94% of conversion in 1.1 h (entry 17). This fact can be
4 ascribed to the steric effect of the bulky substituent. Noteworthy, complete selectivity to the
5 β -(*Z*)-vinylsilane derivative was attained in the hydrosilylation of the substituted
6 phenylacetylene derivatives with R = -CH₃ and -CF₃, and selectivities as high as 94% and 98%
7 for the phenylacetylene derivatives with R = -OMe and -*t*Bu (entries 15, 17, 19 and 21).
8
9

10
11
12 In full agreement with the previous observations, the hydrosilylation of substituted
13 phenylacetylene derivatives with HSiEt₃ required longer reaction times. The reaction of the
14 derivatives with R = -Me, -*t*Bu and -OMe (entries 16, 18 and 20) proceeds faster than with
15 phenylacetylene with conversions in the range of 60-87% in 4 h. As it may be expected, the
16 derivative with R = -CF₃ shows a lower conversion rate, *i.e.* 55% in 24 h (entry 22). As far as
17 the selectivity is concerned, the hydrosilylation of the derivative with R = -CF₃ gave a 90% of
18 selectivity for the β -(*Z*)-vinylsilane isomer. However, moderate selectivity values of 69% and
19 51% were obtained for the derivatives with R = -Me and -*t*Bu, respectively. In sharp contrast,
20 the hydrosilylation of the derivative with R = -OMe gave an 87% of selectivity for the opposite
21 β -(*E*)-vinylsilane stereoisomer.
22
23
24
25
26
27
28
29
30
31
32
33
34
35
36

37 The reaction selectivity is also influenced by the catalyst ability to promote isomerization
38 reactions once the alkyne substrate has been consumed. Both, the β -(*Z*)-vinylsilane
39 isomerization to the more thermodynamically stable β -(*E*)-vinylsilane isomer, and to the
40 corresponding allyl-silyl derivatives in the case of linear alkyl chain alkynes, have been
41 frequently observed.^{3,16d-f,28}
42
43
44
45
46
47
48

49 Although catalyst precursor **1** did not show any substantial isomerization activity for aliphatic
50 alkynes at reasonable reaction times after the consumption of the alkyne, the β -(*Z*) \rightarrow β -(*E*)
51 vinylsilane isomerization process strongly influences the final selectivity in the case of aromatic
52 alkynes, such as phenylacetylene. The monitoring of the hydrosilylation of phenylacetylene
53 with HSiEt₃ by ¹H NMR showed that the reaction was almost completed in 9.5 hours with 83%
54 of selectivity to β -(*Z*)-vinylsilane and a β -(*Z*)/ β -(*E*) ratio of 8.3 (Table 2, entry 15). However,
55
56
57
58
59
60

we have found that **1** slowly promotes the β -(Z) \rightarrow β -(E) vinylsilane isomerization, since the selectivity for β -(Z)-vinylsilane dropped to 46% after 48 h and 3% after 96 h as a consequence of the isomerization process. The extent of this isomerization process can be followed by the evolution of the β -(Z)/ β -(E) ratio along the reaction time (see Figure 2). In contrast with HSiEt₃, when HSiMe₂Ph is chosen as the hydrosilane, the β -(Z) \rightarrow β -(E) vinylsilane isomerization process for the phenylacetylene hydrosilylation did not take place, and the β -(Z)/ β -(E) ratio remains very high at reasonable reaction times after reaction completion.

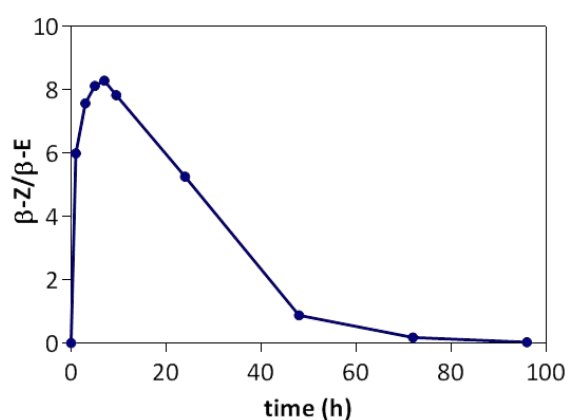


Figure 2. β -(Z)/ β -(E) ratio for the hydrosilylation of phenylacetylene with HSiEt₃ catalyzed by **1** in CDCl₃ at 333 K.

In order to rationalize these results, the hydrosilylation of 4-Me-C₆H₄-C \equiv CH and 4-MeO-C₆H₄-C \equiv CH with HSiEt₃ was monitored by ¹H NMR. As can be seen in the reaction profile of the hydrosilylation of (4-methylphenyl)acetylene with HSiEt₃ (Figure 3), the β -(Z) \rightarrow β -(E) isomerization takes place along the reaction course before the consumption of the substrates. The amount of β -(Z)-vinylsilane isomer increased up to a maximum of 63% at approximately 90% alkyne conversion and then, steadily diminishes. The β -(Z)/ β -(E) ratio progressively reduces from 27.0, 10.0 and 2.4 at 67%, 90% and 95% conversion, respectively. The isomerization of the β -(Z) into the β -(E)-vinylsilane isomer is complete after 48h.

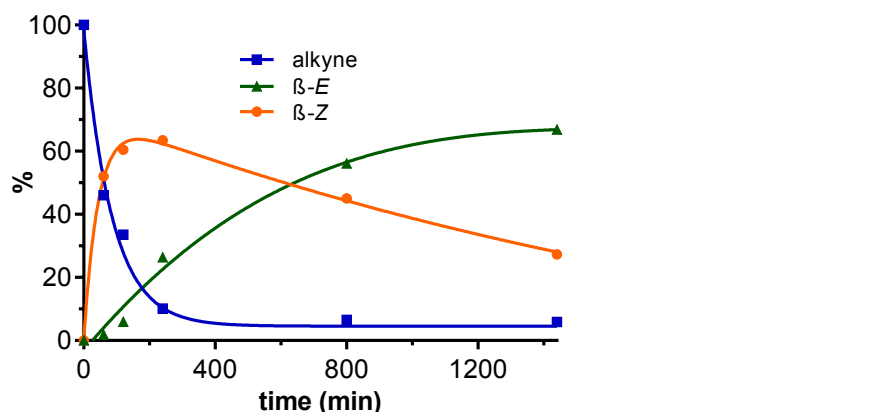


Figure 3. Reaction profile for the hydrosilylation of (4-methylphenyl)acetylene with HSiEt_3 catalyzed by **1** in CDCl_3 at 333 K.

The reaction profile of the hydrosilylation of (4-methoxyphenyl)acetylene with HSiEt_3 also suggests a fast β -(Z) \rightarrow β -(E) isomerization (see Supporting Information). In this case, in the early stage of the reaction both vinylsilane isomers are produced at approximately the same rate. However, after a maximum of 37% (67% alkyne conversion) the amount of β -(Z)-vinylsilane decreases. The β -(Z)/ β -(E) ratio progressively diminishes from 4.5, 1.2 and 0.2 at 67%, 90% and 97% conversion, respectively. As in the precedent case, the isomerization of the β -(Z) into the β -(E)-vinylsilane isomer is almost complete after 24h.

Hydrosilylation of 1-alkynes catalyzed by 1: the role of the carboxylate function. In order to ascertain the impact of the carboxylate function on the catalytic activity of $[\text{Cp}^*\text{RhCl}\{(\text{MeIm})_2\text{CHCOO}\}]$ (**1**), the performance of three related complexes was investigated (Chart 2). Compound $[\text{Cp}^*\text{RhCl}\{(\text{MeIm})_2\text{CHCOOCH}_3\}]^+$ (**6**) has a methoxycarbonyl function at the linker of the bis-NHC ligand, whereas the cationic complex $[\text{Cp}^*\text{RhI}\{(\text{MeIm})_2\text{CH}_2\}]^+$ (**8**) features an unfunctionalized bis-NHC ligand. On the other hand, unlike compound **1** the carboxylate function in the hydrido-iridium(III) complex $[\text{IrH}(\text{cod})\{(\text{MeIm})_2\text{CHCOO}\}]^+$ (**7**) is coordinated to the metal center.

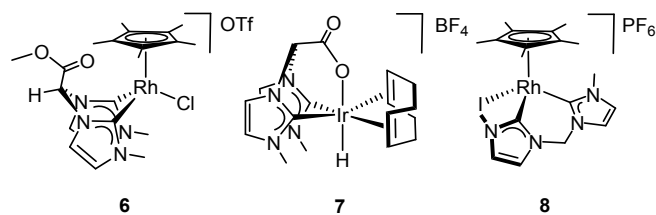
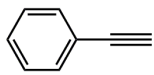
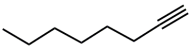


Chart 2. Related catalyst precursors having carboxylate-functionalized and unfunctionalized bis-NHC ligands.

The results of the different hydrosilylation tests are reported in Table 4. The rhodium(III)-based compound **6**, which features an alkoxy carbonyl functional group at the bis-NHC ligand, is less active than **1** in the hydrosilylation of both phenylacetylene and oct-1-yne (entries 2 and 6). Namely, the reaction with oct-1-yne provides a 73% selectivity for β -(*Z*)-vinylsilane although reverse selectivity was observed with phenylacetylene giving a 62% selectivity for the β -(*E*)-vinylsilane isomer. Moreover, the hydrido-iridium(III) compound **7**, in addition to be less active than **1**, has been found to be completely non-selective (entries 3 and 7). Unexpectedly, catalyst precursor **8** did not exhibit any catalytic activity at all in alkyne hydrosilylation under the same reaction conditions (entries 4 and 8).

The previously explained results have shown that $[\text{Cp}^*\text{RhCl}\{(\text{MeIm})_2\text{CHCOO}\}]$ (**1**) is an efficient catalyst precursor for the hydrosilylation of a range of terminal alkynes with excellent regio- and stereoselectivity towards the less thermodynamically stable β -(*Z*)-vinylsilane isomer. In contrast, the inactivity of catalyst precursor $[\text{Cp}^*\text{RhI}\{(\text{MeIm})_2\text{CH}_2\}]^+$ (**8**) and the lower catalytic performance of compound $[\text{Cp}^*\text{RhCl}\{(\text{MeIm})_2\text{CHCOOCH}_3\}]^+$ (**6**) strongly suggests that the carboxylate function in **1** plays a key role in the reaction mechanism. Moreover, the poor selectivity and activity of compound $[\text{IrH}(\text{cod})\{(\text{MeIm})_2\text{CHCOO}\}]^+$ (**7**), with the functionalized bis-NHC ligand κ^3 -*C,C',O*-coordinated, also indicates that the carboxylate function is not likely to be engaged in the coordination to the metal center and that its action is crucial for the reaction to take place.

Table 4. Hydrosilylation of terminal alkynes with HSiMe₂Ph catalyzed by bis-NHC rhodium, iridium and ruthenium complexes.^{a,b}

entry	alkyne	catalyst	time (h)	conv. (%)	β-(Z) (%)	β-(E) (%)	α (%)	alkene (%)
1		1	0.4	>99	>99	---	---	---
2		6	7	85	8	62	4	26
3		7	24	>99	29	25	18	28
4		8	24	0	---	---	---	---
5		1	0.4	>99	>99	---	---	---
6		6	4	96	73	17	2	8
7		7	24	90	5	17	21	57
8		8	24	0	---	---	---	---

a) Experiments were carried out in CDCl₃ at 333 K using a HSiMe₂Ph/RC≡CH/catalyst ratio of 100/100/1, [catalyst] = 1.54 mM. b) Conversion and selectivities determined by ¹H NMR using anisole as internal standard.

Mechanistic studies on the hydrosilylation of 1-alkynes catalyzed by 1. In the search for a deeper understanding of the operating mechanism for the hydrosilylation of terminal alkynes and the role of the carboxylate group in [Cp**Rh*Cl{(MeIm)₂CHCOO}] (**1**), we have performed an in-depth study on the basis of theoretical calculations and some specific experiments. This way, we carried out a complete mechanistic study by using Density Functional Theory (DFT) at the B3LYP-D3BJ(PCM, chloroform)/def2-TZVP// B3LYP-D3BJ/def2-SVP level of theory, as explained in the Experimental section. The complete structure of the catalyst precursor **1** was considered in the calculations, without any structural simplification, due to the presence of the pentamethylcyclopentadienyl ligand or the carboxylate function which can influence the catalyst mode of action.^{14,29} The most reactive reductant, HSiMe₂Ph, was selected as the hydrosilane model, while phenylacetylene was the chosen alkyne. For the sake of clarity, the

reaction intermediates and transition states are referred to by means of capital letters, starting from **A**, which corresponds to structure **1**.

In accordance with classical mechanisms, the two possible initial reactions entail prior coordination of the alkyne to give a vinylidene or the oxidative addition of the silane.^{30,31} However, both reactions pathways can be excluded as **1** is apparently unreactive towards alkynes and hydrosilanes, even at high temperatures up to 333 K for 24 hours. Moreover, the experimental data suggests that the carboxylate fragment in the zwitterionic complex $[\text{Cp}^*\text{RhCl}\{(\text{MeIm})_2\text{CHCOO}\}]$ (**1**) should actively participate in the hydrosilylation mechanism. Thus, we envisaged a mechanistic proposal where the carboxylate fragment acts as a silane carrier, the proposal being shown in Figure 4.

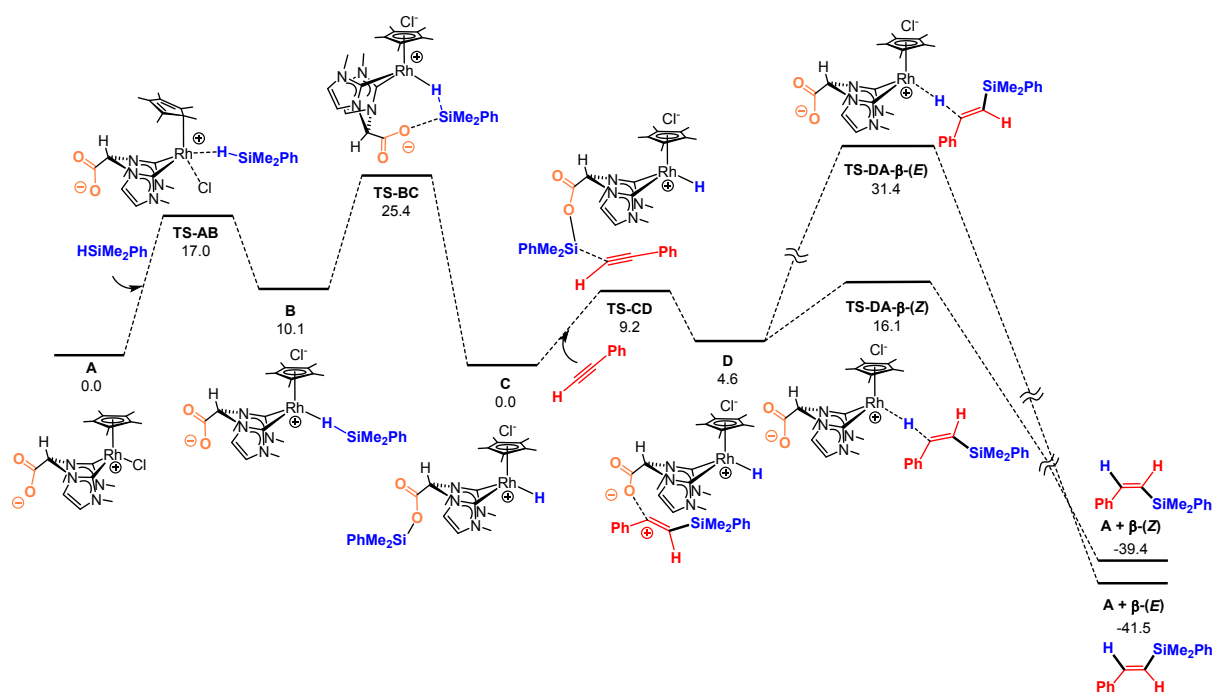


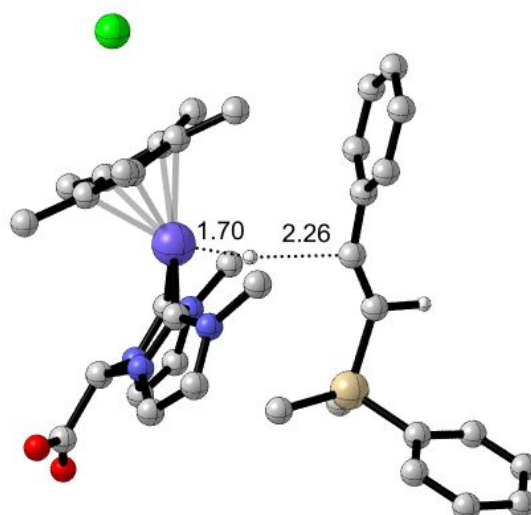
Figure 4. DFT calculated Gibbs free energy profile (in kcal·mol⁻¹) relative to **A** and the isolated molecules. Note that for visual purposes the energy diagram is not at a scale.

The first step consists on the ligand exchange between the chlorido ligand and the hydrosilane, yielding intermediate **B**, with a relative Gibbs energy of 10.1 kcal·mol⁻¹. This process requires to overcome an energy barrier of 17.0 kcal·mol⁻¹, dictated by transition

1
2
3 structure **TS-AB**, which is feasible under the reaction conditions (RT and 333 K). Remarkably,
4 within **TS-AB** the Cp* ligand changes its coordination mode from η^5 to η^1 , as we previously
5 proposed for the related complex $[\text{Cp}^*\text{IrCl}\{(\text{MeIm})_2\text{CHCOO}\}]$,²² and which is enabled by the
6 flexibility in the coordination modes of the pentamethylcyclopentadiene ligand.^{32,33,34} The next
7 step involves the hydrosilane activation through a ligand assisted Si–H bond cleavage process,
8 in line with other activation proposals for similar Ir-based catalysts.^{29,35} This step leads to
9 intermediate **C** and involves the formation of a Si–O bond in the carboxylate moiety and a Rh–
10 H bond. This species has a relative energy of 0.0 kcal·mol⁻¹, being 10.1 kcal·mol⁻¹ more stable
11 than **B** as a consequence of the high oxophilicity of silicon, which favors the formation of the
12 Si–O bond. This process bears an energy barrier of 25.4 kcal·mol⁻¹ (with respect to **A**). At this
13 point, it is important to mention that we also explored the oxidative addition of the hydrosilane
14 and the alkyne to the metal center, as it would be the case in a “classical” inner-sphere
15 mechanism; however, in agreement with the experimental observations, we could not find any
16 stable reaction product. We attribute this result to the fact that **A** (catalyst precursor **1**) bears a
17 Rh(III) center, and thus the oxidative addition of the hydrosilane or the alkyne would result into
18 a Rh(V) intermediate. These kind of intermediates have extensively been reported to be
19 unstable, as it was the case in the species under study, and there are very few examples in the
20 literature.³⁶

21
22
23
24
25
26
27
28
29
30
31
32
33
34
35
36
37
38
39
40
41
42
43
44
45 The next step consists on the alkyne activation, which was revealed to take place by means
46 of the direct transference of the Me₂PhSi⁺ moiety from the carboxylate group to the α carbon
47 of the alkyne, *via* transition structure **TS-CD**. This step needs to surmount an energy barrier of
48 9.2 kcal·mol⁻¹, as dictated by the energy difference between **TS-CD** and intermediate **C**. As a
49 result, a β -silyl carbocation intermediate (structure **D**), with a relative energy of 4.6 kcal·mol⁻¹,
50 is generated. We attribute its relative high stability to be a consequence of the large
51 hyperconjugative nature of the β -silyl effect.³⁷ Then, as a final step, the β -silyl carbocation
52 reacts selectively with the hydrido complex. Namely, it undergoes a hydride transfer from the
53
54
55
56
57
58
59
60

1
2
3 Rh(III) center and generates the vinylsilane product, thus closing the catalytic cycle and
4 recovering **A**. Notice that, along this process, the carboxylate moiety does not have to flip (as
5 it happened in **TS-BC**) because its role consists just on transferring the silane to the alkyne for
6 the generation of the carbocation, without having any direct interaction with the hydride ligand.
7
8 This way, the vinylsilane is formed by nucleophilic attack of the hydride over the carbocation.
9
10 and the catalytic cycle is closed by coordination of silane to the metal center. Remarkably, there
11
12 are two different possibilities for the aforementioned attack, depending on whether the Me_2PhSi
13 moiety points towards the metal complex (**TS-DA- β (E)**) or outside the complex (**TS-DA- β (Z)**),
14 see Figure 5. Notice that **TS-DA- β (E)** would lead to the β (E)-vinylsilane, while **TS-DA- β (Z)**
15 would lead to the β (Z)-vinylsilane. **TS-DA- β (Z)** is $11.7 \text{ kcal}\cdot\text{mol}^{-1}$ more stable than **TS-DA-**
16 **β (E)**, explaining the outstanding selectivity towards the β (Z)-vinylsilane, which is a
17 consequence of the lower steric repulsion between the Me_2PhSi^+ moiety and the Cp^* ligand in
18 **TS-DA- β (Z)**. The energy barrier for that process (taken from intermediate **C**) is $19.7 \text{ kcal}\cdot\text{mol}^{-1}$
19 for the β (Z)-vinylsilane, making it feasible under the reaction conditions. Also notice that the
20 final step is very exergonic, as the final β (Z)-vinylsilane product plus the original catalyst are
21 $44.0 \text{ kcal}\cdot\text{mol}^{-1}$ more stable than **D**.



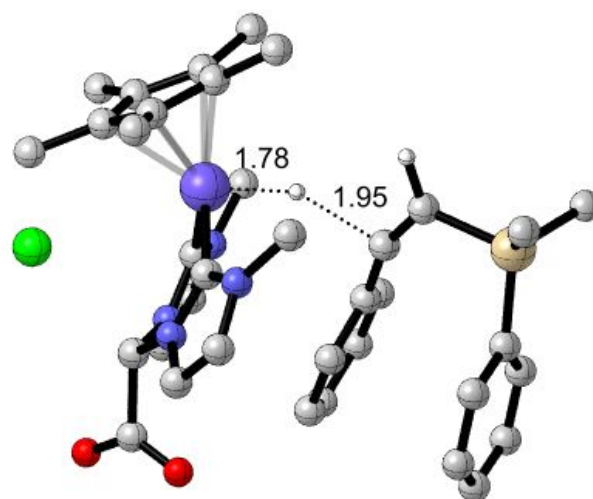


Figure 5. Geometrical representation of DFT calculated **TS-DA- $\beta(E)$** (up) and **TS-DA- $\beta(E)$** (down). Key distances in Å.

Overall, the whole process has a ΔG of $-39.4 \text{ kcal}\cdot\text{mol}^{-1}$, thus being highly thermodynamically favorable. It features an effective energy span of $25.4 \text{ kcal}\cdot\text{mol}^{-1}$ according to the model proposed by Kozuch *et al.*³⁸ This barrier is determined by the Gibbs energy difference between **TS-BC** and **A**, which corresponds to the hydrosilane activation (*i.e.* the ligand assisted Si–H bond cleavage). It is also remarkable that the original catalyst precursor (structure **A**, also referred to as **1**) is recovered at the end of the cycle, discarding the need for any pre-activation process. The proposed reaction mechanism also unravels the key role of the carboxylate function. In particular, it acts as the shuttle that transfers the silane moiety to the alkyne, yielding the β -silyl carbocation (intermediate **D**) that will eventually lead to the final product. Such functionality is also of essential importance in the reaction selectivity, as it enables the formation of a flat carbocation intermediate (**D**), which would further evolve to the $\beta(Z)$ -vinylsilane so as to minimize the steric repulsion in the hydride transfer transition state (**TS-DA**). In this regard, we previously reported that the $[\text{Ml}_2\{\kappa^4\text{-C,C,O,O-(bis-NHC)}\}]\text{BF}_4$ ($\text{M} = \text{Rh, Ir}$; bis-NHC = methylenebis(N-2-methoxyethyl)imidazole-2-ylidene) complex is

1
2
3 able to selectively generate the $\beta(Z)$ -vinylsilane thanks to the presence of acetone in the reaction
4
5 medium.¹⁷ This molecule was revealed by theoretical and experimental studies to be the silane
6
7 shuttle that transfers such function to the alkyne. Herein, we propose that this role is played by
8
9 the carboxylate group. Moreover, the lack of selectivity and much lower catalytic activity of
10
11 compounds **6**, **7** and **8** (see Chart 2), in which the uncoordinated carboxylate group has been
12
13 eliminated, adds additional evidence to the proposed role of the carboxylate function in the
14
15 catalytic activity and selectivity, and thus to the consistency of the proposed reaction
16
17 mechanism.
18
19
20

21
22 It is worth mentioning that although the role of carboxylate as an oxygen-nucleophile for
23
24 hydrosilane activation is well documented, to the best of our knowledge, the heterolytic
25
26 hydrosilane splitting into silyl carboxylate and metal hydride had not been previously
27
28 described.³⁹ In this context, silyl formates has been reported as surrogates of hydrosilanes for
29
30 transfer hydrosilylation of aldehydes in the presence of a well-defined ruthenium catalyst.⁴⁰
31
32

33
34 In order to shed light on the feasibility of the catalytic cycle, we performed the hydrosilylation
35
36 of deuterated phenylacetylene with HSiMe₂Ph and studied it by means of ¹H NMR in CDCl₃.
37
38 The hydrosilylation of PhC≡C-D resulted in the exclusive formation of the (*Z*)-
39
40 dimethyl(phenyl)(2-phenylvinyl-1-*d*)silane product (see Supporting Information) thereby
41
42 confirming the lack of H/D scrambling. This compound was unambiguously identified by the
43
44 lack of the vinyl resonance at δ 6.03 ppm and the virtual triplet at δ 7.51 ppm ($J_{H-D} = 1.9$ Hz),
45
46 due to the coupling of the vinyl proton at C₂ with the *cis*-disposed deuterium atom. The
47
48 percentage of deuterium in the product is in agreement with the deuteration degree of PhC≡C-
49
50 D (97%). This result also agrees with the DFT outcome. Namely, the D atom of
51
52 phenylacetylene-*d*₁ would correspond to the hydrogen atom depicted in red in Figure 4, which
53
54 remains at the C₁ carbon of the final $\beta(Z)$ -vinylsilane product. The lack of deuterium scrambling
55
56 in the product rules out the preliminary activation of the alkyne (e.g. vinylidene formation), and
57
58 suggests that reaction proceeds through the hydrosilane activation, as shown by the DFT study.
59
60

We also analyzed the mass spectra of the catalytic solution resulting from the hydrosilylation of phenylacetylene with HSiMe₂Ph catalyzed by **1**. The ESI-MS mass spectrum of the solid recovered from the catalytic solution after diethyl ether addition, which could be the resting state of the catalyst, showed three main peaks at *m/z* 493.1 (42%), 629.2 (6%) and 763.2 (100%) (Figure 6).

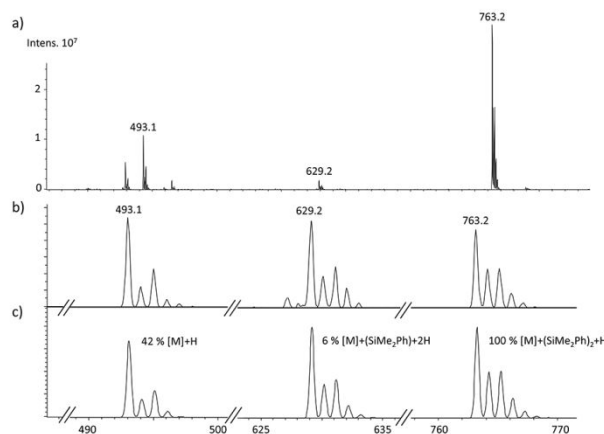


Figure 6. ESI+ mass spectrum (CHCl₃) of the isolated solid after hydrosilylation of phenylacetylene with HSiMe₂Ph catalyzed by **1**: a) full spectrum, b) observed, and c) calculated isotopic distribution patterns for the main species.

Interestingly, the isotopic distribution of these peaks is in full agreement with the following rhodium species: the peak at *m/z* 763.2 (100%) corresponds to the rhodium catalyst precursor with two SiMe₂Ph fragments and one hydrogen atom, whereas the peaks at *m/z* 629.2 (6%) and *m/z* 493.1 (42%) result from the sequential loss of the two SiMe₂Ph fragments from the former. Remarkably, the species at *m/z* 629.2 may well correspond to intermediate **C**, which is a significantly stable reaction intermediate according to the theoretical calculations and has the same molecular mass. Moreover, the peak at *m/z* 493.1 is consistent with intermediate **D**, from which the vinyl-carbocation moiety has been eliminated, as expected for positively charged species in the mass spectrometer. We attribute the observation of a doubly silylated species at *m/z* 763.2 to be a consequence of the molecular processes that may take place in the mass

1
2
3 spectrometer environment, which are in many cases different from those observed in solution
4
5 as a consequence of the very different conditions.⁴¹
6
7

8 CONCLUSIONS

9

10 The catalytic activity towards alkyne hydrosilylation of a series of zwitterionic rhodium,
11 iridium and ruthenium [Cp*MCl{(MeIm)₂CHCOO}], [M(cod){(MeIm)₂CHCOO}] (M = Rh,
12 Ir) and [(*p*-cymene)RuCl{(MeIm)₂CHCOO}] compounds has been investigated using the
13 hydrosilylation of phenylacetylene and oct-1-yne with HSiMe₂Ph as model reaction under mild
14 conditions. The rhodium(III) compound [Cp*RhCl{(MeIm)₂CHCOO}] is by far the most
15 active one giving full conversion to the β-(*Z*)-vinylsilane product. The outstanding
16 stereoselectivity is maintained both at room temperature and low catalyst loading.
17
18
19
20
21
22
23
24
25

26 Compound [Cp*RhCl{(MeIm)₂CHCOO}] has proven to be an efficient catalyst for the
27 hydrosilylation of a range of aliphatic and aromatic terminal alkynes. Hydrosilylation of linear
28 1-alkynes, cycloalkyl acetylenes and aromatic alkynes with HSiMe₂Ph selectively affords the
29 β-(*Z*)-vinylsilane product in very short reaction times. The reaction of aliphatic alkynes with
30 HSiEt₃ is slower, which results in a slight decrease of selectivity. The efficiency of the
31 hydrosilylation of aromatic alkynes is influenced by the electronic and steric effects of the
32 substituent at the phenyl ring. A clear cut off is found in the hydrosilylation of aromatic alkynes
33 with HSiEt₃, electron-donating substituents at the *para* position increase the catalytic activity
34 whereas the opposite effect is observed for electron-withdrawing substituents. However, in this
35 case, the selectivity for the β-(*Z*)-vinylsilane products is lost due to the β-(*Z*)→β-(*E*)
36 isomerization process that takes places upon the vinylsilane formation. This is especially
37 remarkable in the hydrosilylation of derivatives bearing electron-donating substituents. On the
38 other hand, the hydrosilylation of bulky alkynes such as *t*-Bu-C≡CH and Et₃SiC≡CH with either
39 HSiMe₂Ph or HSiEt₃ was unselective.
40
41
42
43
44
45
46
47
48
49
50
51
52
53
54
55
56
57
58

59 The outstanding catalytic performance of [Cp*RhCl{(MeIm)₂CHCOO}] contrasts with that
60 of [Cp*RhI{(MeIm)₂CH₂}]⁺, a related cationic compound featuring an unfunctionalized bis-

1
2
3 NHC ligand, which is completely inactive under the same reaction conditions. This suggests
4 that the carboxylate function plays a key role of in the reaction mechanism. In this regard, the
5 application of DFT calculations has allowed to propose a plausible ionic outer-sphere
6 mechanism pathway. According to our proposal, the carboxylate fragment acts as a silane
7 carrier and explains the excellent β -(Z) selectivity outcome of the hydrosilylation reactions. The
8 first step involves the heterolytic activation of the hydrosilane assisted by the carboxylate
9 function to give the hydrido intermediate $[\text{Cp}^*\text{RhH}\{(\text{MeIm})_2\text{CHCOO-SiR}_3\}]^+$, which features
10 a silyl-carboxylate functionalized bis-NHC ligand. Then, the direct transference of the R_3Si^+
11 moiety from the carboxylate group to the alkyne results in the formation of a flat β -silyl
12 carbocation intermediate that undergoes a hydride transfer from the Rh(III) center to generate
13 the vinylsilane product. The minimization of the steric repulsions in the hydride transfer
14 transition state explains the observed selectivity for the β -(Z)-vinylsilane product. This proposal
15 is substantiated by labelling studies involving $\text{PhC}\equiv\text{C-D}$, which rules out a possible alkyne
16 activation pathway. Finally, ESI+ mass spectroscopy has allowed to identify some of the
17 species that are in agreement with those proposed in the catalytic cycle, such as the key hydrido
18 intermediate.

41 42 43 **EXPERIMENTAL**

44
45 **General Considerations.** All the experimental procedures were performed under argon
46 atmosphere by using Schlenk or glovebox techniques. Solvents were taken under argon
47 atmosphere from an Innovative Technologies solvent purification system (SPS) or dried
48 following standard procedures and distilled under argon prior to use. CDCl_3 and CDCl_2 (Euriso-
49 top) were dried using activated molecular sieves and degassed by three freeze-pump-thaw
50 cycles. The zwitterionic compounds $[\text{Cp}^*\text{MCl}\{(\text{MeIm})_2\text{CHCOO}\}]$ (M = Rh, **1**; Ir, **2**),
51 $[\text{Cp}^*\text{RuCl}\{(\text{MeIm})_2\text{CHCOO}\}]$ (**3**) and $[\text{M}(\text{cod})\{(\text{MeIm})_2\text{CHCOO}\}]$ (M = Rh, **4**; Ir, **5**), and
52 complexes $[\text{Cp}^*\text{RhCl}\{(\text{MeIm})_2\text{CHCOOCH}_3\}]\text{OTf}$ (**6**) and $[\text{IrH}(\text{cod})\{(\text{MeIm})_2\text{CHCOO}\}]\text{BF}_4$
53
54
55
56
57
58
59
60

1
2
3 (7) were prepared following the procedures recently reported by us.^{19,21} Deuterated
4 phenylacetylene, PhC≡CD, was prepared according to the literature procedure.⁴² All other
5 reagents were commercially available and used as received.
6
7

8
9
10 **Scientific Equipment.** ¹H and ¹³C{¹H} NMR spectra were recorded on Bruker Avance
11 spectrometers (300, 400 or 500). Chemical shifts are reported in ppm relative to
12 tetramethylsilane and referenced to partially deuterated solvent resonances. Coupling constants
13 (*J*) are given in Hertz (Hz). Electrospray ionization (ESI) mass spectra were recorded using a
14 Bruker Esquire3000 plus™ ion-trap mass spectrometer equipped with a standard ESI source.
15 Gas chromatography/mass spectrometry (GC/MS) analyses were performed on an Agilent 7673
16 GC autosampler system with an Agilent 5973 MS detector operating in EI ionization method
17 at 70 eV, equipped with an Phenomenex ZB-5HT apolar capillary column (0.25 μm film
18 thickness, 30 m × 0.25 mm i.d.).
19
20
21
22
23
24
25
26
27
28
29

30
31 **Synthesis of [Cp*RhI{(MeIm)₂CH₂}]PF₆ (8).**⁴³ The compound was prepared following an
32 one-pot procedure according to the synthetic method described by Heinekey and co-workers
33 for the analogous iridium complex.⁴⁴ AgPF₆ (334.8 mg, 1.324 mmol) was added to a solution
34 of [Cp*RhCl₂]₂ (204.6 mg, 0.331 mmol) in acetonitrile (5 mL) and the mixture stirred for 4
35 hours at room temperature. The resulting yellow suspension was filtered through Celite to
36 remove the silver salt formed to give a yellow solution. The addition of [(MeIm)₂CH₂]₂I₂ (286.2
37 mg, 0.662 mmol) gave an orange suspension which turned into red whereupon the addition of
38 NE₃ (185.5 μL, ρ = 0.726 g·mL⁻¹, 99.5%, 1.324 mmol). The red suspension was heated at 333
39 K for 48 h to give a dark orange solution. The solution was cooled to room temperature and the
40 solvent was removed under vacuum. The addition of CHCl₃ (5 mL) resulted in a yellow
41 suspension which was decanted and then filtered. The yellow solid was washed with methanol
42 (2 x 5 mL) and diethyl ether (3 x 3 mL), and dried in vacuo. Yield: 308.9 mg, 68%. Anal. Calc.
43 for C₁₉H₂₇F₆IN₄PRh: C, 33.25; H, 3.97; N, 8.16. Found: C, 32.91; H, 3.96; N, 8.11. ¹H NMR
44 (298 K, 400 MHz, CD₂Cl₂): δ 7.35 (d, *J*_{H-H} = 1.3, 2H, CH), 7.07 (d, *J*_{H-H} = 1.2, 2H, CH), 6.13
45
46
47
48
49
50
51
52
53
54
55
56
57
58
59
60

(d, $J_{\text{H-H}} = 13.3$, 1H, NCH₂N), 5.64 (d, $J_{\text{H-H}} = 13.3$, 1H, NCH₂N), 3.74 (s, 6H, NCH₃), 1.81 (s, 15H, CH₃ Cp*). ¹³C{¹H} NMR (298 K, 101 MHz, CD₂Cl₂): δ 167.0 (d, $J_{\text{C-Rh}} = 51.6$, C_{NCN}), 124.3, 123.0 (CH), 100.2 (d, $J_{\text{C-Rh}} = 5.1$, CCH₃ Cp*), 62.1 (NCH₂), 41.3 (NCH₃), 10.5 (CH₃ Cp*). HRMS (ESI+, CH₂Cl₂/MeOH, m/z, %): 541.0 ([M]⁺, 100).

General procedure for catalytic alkyne hydrosilylation reactions. Hydrosilylation catalytic tests were carried out in NMR tubes, under an argon atmosphere in CDCl₃. In a typical procedure, a NMR tube was charged under argon with the catalyst (7.7×10^{-4} mmol, 1 mol %), CDCl₃ (0.5 mL), the corresponding alkyne (0.077 mmol), hydrosilane (0.077 mmol) and anisole (7.7×10^{-3} mmol) as internal standard. The solution was kept at room temperature or in a thermostated bath at 298 K or 333 K and monitored by ¹H NMR spectroscopy. Yields and selectivities were calculated by ¹H NMR spectroscopy. The reaction products were unambiguously characterized on the basis of the ³ $J_{\text{H-H}}$ coupling constants of the vinylic protons in the ¹H NMR spectra and subsequent comparison to literature values.^{3a,45} Values for J ranged from 17 to 19 Hz for β -(*E*), 13 to 16 Hz for β -(*Z*), and 1 to 3 Hz for α -vinyldisilanes. Hydrosilylation of 1-octene with HSiMe₂Ph in water was performed in a schlenk tube with vigorously stirring following the same procedure described before. After 24 reaction time the organics were extracted with diethyl ether and dried under vacuum to give a yellow oil. Reaction products were identified by ¹H NMR (CDCl₃).

Hydrolysis of HSiMe₂Ph catalyzed by 1. Water (5 mmol) was added to a NMR tube containing a solution of **1** (0.01 mmol) and HSiMe₂Ph (0.1 mmol) in CDCl₃. Monitoring of the reaction by ¹H NMR evidenced the steady consumption of the hydrosilane with formation of siloxane (PhMe₂Si)₂O⁴⁶ and H₂(g) evolution (see Supporting Information). ¹H NMR (298 K, 400 MHz, CDCl₃): δ 7.60-7.37 (m, 10 H, Ph), 0.37 (s, 12H, Me). ¹³C{¹H} NMR (298 K, 101 MHz, CDCl₃): δ 140.0, 133.1, 129.4, 127.9, (Ph), 1.0 (Me). ¹H-²⁹Si HMQC (298 K, 101 MHz, CDCl₃): δ -1.1 (s).

1
2
3 **Computational details.** DFT calculations were performed using the Gaussian09 software
4 package, D.01revision.⁴⁷ The energies and gradient calculations were computed by using the
5 B3LYP exchange-correlation functional,⁴⁸ in conjunction with the D3BJ dispersion correction
6 scheme developed by Grimme *et al.*⁴⁹ We also set the “ultrafine” grid. The def2-SVP basis set
7 was used for all the atoms in geometry optimization, and energies were further refined through
8 single point calculations using the def2-TZVP basis set.⁵⁰ Solvent corrections were included by
9 means of the PCM model (chloroform), as implemented in the G09 package.⁵¹ The Gibbs
10 energies reported herein were obtained within the framework proposed by Morokuma and co-
11 workers, i.e. we removed the translational entropy contribution from dissolved species.⁵² The
12 nature of the stationary points has been confirmed by analytical frequencies analysis.

26 **ASSOCIATED CONTENT**

27
28 **Supporting Information.** NMR monitoring of selected hydrosilylation reactions and
29 hydrosilane hydrolysis and deuterium labelling studies, DFT energy data and optimized
30 coordinates for catalytic intermediates and transition states (XYZ). The Supporting Information
31 is available free of charge on the ACS Publications website at DOI: #####.

36 **ACKNOWLEDGMENTS**

37
38 The authors express their appreciation for the financial support from the Spanish Ministry of
39 Economy and Competitiveness MINECO/FEDER under the project CTQ2016-75884-P and the
40 Regional Governments of Aragón/FEDER 2014-2020 “*Building Europe from Aragón*” (group
41 E42_17R). In addition, the resources from the supercomputer “Memento”, technical expertise
42 and assistance provided by BIFIZCAM (Universidad de Zaragoza) are acknowledged.

46 **AUTHOR INFORMATION**

47 **Corresponding Authors**

48
49 Jesús J. Pérez-Torrente: perez@unizar.es

1
2
3 M. Victoria Jiménez: vjimenez@unizar.es
4
5

6 **Author Contributions**

7

8 The manuscript was written through contributions of all authors. All authors have given
9 approval to the final version of the manuscript.
10
11
12

13 **ORCID**

14
15
16 Julen Munarriz: 0000-0001-6089-6126

17
18 Víctor Polo: 0000-0001-5823-7965

19
20 M. Victoria Jiménez: 0000-0002-0545-9107

21
22 Jesús J. Pérez-Torrente: 0000-0002-3327-0918
23
24

25 **Funding Sources**

26

27 Any funds used to support the research of the manuscript should be placed here (per journal
28 style).
29
30
31
32
33
34
35

36 **REFERENCES**

37
38
39

- 40 (1) (a) Ojima, I.; Li, Z.; Zhu, J. In *The Chemistry of Organic Silicon Compounds*;
41 Rappoport, Z., Apeloig, Y., Eds.; Wiley: New York, 1998; Vol. 2, pp 1687–1792. (b)
42 Komiyama, T.; Minami, Y.; Hiyama, T. Recent Advances in Transition-Metal-Catalyzed
43 Synthetic Transformations of Organosilicon Reagents. *ACS Catal.* **2017**, *7*, 631–651. (c)
44 Szudkowska-Frątczak, J.; Hreczycho, G.; Pawluć, P. Silylative coupling of olefins with
45 vinylsilanes in the synthesis of functionalized alkenes. *Org. Chem. Front.* **2015**, *2*, 730–738.
46
47 (d) Lim, D. S. W.; Anderson, E. A. Synthesis of Vinylsilanes. *Synthesis* **2012**, *44*, 983–1010.
48
49 (e) Denmark, S. E.; Ober, M. H. Organosilicon Reagents: Synthesis and Application to
50 Palladium-Catalyzed Cross-Coupling Reactions. *Aldrichimica Acta* **2003**, *36*, 75–85.
51
52
53
54
55
56
57
58
59
60

1
2
3
4
5
6 (2) (a) Marciniak, B., Maciejewski, H., Pietraszuk, C. and Pawluć, P. Hydrosilylation and
7 Related Reactions of Silicon Compounds. In *Applied Homogeneous Catalysis with*
8 *Organometallic Compounds*; Cornils, B.; Herrmann, W. A.; Beller, M.; Paciello, R., Eds.;
9 Wiley-VCH: Weinheim, Germany, 2017, pp. 569–620. (b) Marciniak, B. Hydrosilylation of
10 Alkynes and Their Derivatives. In *Hydrosilylation: A Comprehensive Review on Recent*
11 *Advances*; Marciniak, B., *Advances In Silicon Science*, vol 1. Springer, Dordrecht, 2009; pp
12 53–83. (c) Roy, A. K. A Review of Recent Progress in Catalyzed Homogeneous Hydrosilylation
13 (Hydrosilylation). *Adv. Organomet. Chem.* **2007**, *55*, 1–59.

14
15
16
17
18
19
20
21
22
23
24
25 (3) (a) Pérez-Torrente, J. J.; Nguyen, D. H.; Jiménez, M. V.; Modrego, F. J.; Puerta-Oteo,
26 R.; Gómez-Bautista, D.; Iglesias, M.; Oro, L. A. Hydrosilylation of Terminal Alkynes
27 Catalyzed by a ONO-Pincer Iridium(III) Hydride Compound: Mechanistic Insights into the
28 Hydrosilylation and Dehydrogenative Silylation Catalysis. *Organometallics* **2016**, *35*, 2410–
29 2422. (b) Shimizu, R.; Takamasa F. Dehydrogenative Silylation of Terminal Alkynes by
30 Iridium Catalyst. *Tetrahedron Lett.* **2000**, *41*, 907–910. (c) Jun, C.-H.; Crabtree, R. H.
31 Dehydrogenative Silylation, Isomerization and the Control of Syn- vs. Anti-addition in the
32 Hydrosilylation of Alkynes. *J. Organomet. Chem.* **1993**, *447*, 177–187.

33
34
35
36
37
38
39
40
41
42
43
44 (4) (a) Sánchez-Page, B.; Jiménez, M. V.; Pérez-Torrente, J. J.; Passarelli, V.; Blasco, J.;
45 Subias, G.; Granda, M.; Álvarez, P. Hybrid Catalysts Comprised of Graphene Modified with
46 Rhodium-Based N-Heterocyclic Carbenes for Alkyne Hydrosilylation. *ACS Appl. Nano Mater.*
47 **2020**, *3*, 1640–1655. (b) Zhao, X.; Yang, D.; Zhang, Y.; Wang, B.; Qu, J. Highly β (Z)-Selective
48 Hydrosilylation of Terminal Alkynes Catalyzed by Thiolate-Bridged Dirhodium Complexes.
49 *Org. Lett.* **2018**, *20*, 5357–5361. (c) Mori, A.; Takahisa, E.; Yamamura, Y.; Kato, T.; Mudalige,
50 A. P.; Kajiro, H.; Hirabayashi, K.; Nishihara, Y.; Hiyama, T. Stereodivergent Syntheses of (Z)-
51 and (E)-Alkenylsilanes via Hydrosilylation of Terminal Alkynes Catalyzed by Rhodium(I)

1
2
3
4
5
6 Iodide Complexes and Application to Silicon-Containing Polymer Syntheses. *Organometallics*
7
8 **2004**, *23*, 1755-1765.
9

10
11 (5) (a) Corre, Y.; Werlé, C.; LydiaBrelot-Karmazin, L.; Djukic, J.-P.; Agbossou-Niedercorn,
12 F.; Michon, C. Regioselective hydrosilylation of terminal alkynes using
13 pentamethylcyclopentadienyl iridium(III) metallacycle catalysts. *J. Mol. Catal. A-Chem.* **2016**,
14 *423*, 256–263. (b) Iglesias, M.; Pérez-Nicolás, M.; Sanz Miguel, P. J.; Polo, V.; Fernández-
15 Alvarez, F. J.; Pérez-Torrente, J. J.; Oro, L. A. A synthon for a 14-electron Ir(III) species:
16 catalyst for highly selective β -(Z) hydrosilylation of terminal alkynes. *Chem. Commun.* **2012**,
17 *48*, 9480–9482. (c) Sridevi, V. S.; Fan, W. Y.; Leong, W. K. Stereoselective Hydrosilylation of
18 Terminal Alkynes Catalyzed by $[\text{Cp}^*\text{IrCl}_2]_2$: A Computational and Experimental Study.
19 *Organometallics* **2007**, *26*, 1157–1160.
20
21
22
23
24
25
26
27
28
29
30
31

32
33 (6) (a) Conifer, C.; Gunanathan, C.; Rinesch, T.; Hölscher, M.; Leitner, W. Solvent-Free
34 Hydrosilylation of Terminal Alkynes by Reaction with a Nonclassical Ruthenium Hydride
35 Pincer Complex. *Eur. J. Inorg. Chem.* **2015**, 333–339. (b) Gao, R.; Pahls, D. R.; Cundari, T.
36 R.; Yi, C. S. Experimental and Computational Studies of the Ruthenium-Catalyzed
37 Hydrosilylation of Alkynes: Mechanistic Insights into the Regio- and Stereoselective
38 Formation of Vinylsilanes. *Organometallics* **2014**, *33*, 6937–6944. (c) Na, Y.; Chang, S. Highly
39 Stereoselective and Efficient Hydrosilylation of Terminal Alkynes Catalyzed by $[\text{RuCl}_2(\text{p-}$
40 $\text{cymene})]_2$. *Org Lett.* **2000**, *2*, 1887–1889.
41
42
43
44
45
46
47
48
49
50

51
52 (7) Wen, H.; Liu, G.; Huang, Z. Recent Advances in Tridentate Iron and Cobalt Complexes
53 for Alkene and Alkyne Hydrofunctionalizations. *Coord. Chem. Rev.* **2019**, *386*, 138–153.
54
55
56
57
58
59
60

1
2
3
4
5
6 (8) Liang, H.; Ji, Y.-X.; Wang, R.-H. Zhang, Z.-H.; Zhang, B. Visible-Light-Initiated
7
8
9 Manganese-Catalyzed E-Selective Hydrosilylation and Hydrogermylation of Alkynes. *Org.*
10
11 *Lett.* **2019**, *21*, 2750–2754.

12
13
14
15 (9) (a) Dierick, S.; Vercruyse, E.; Berthon-Gelloz, G.; Markó, I. E. User-Friendly Platinum
16
17
18 Catalysts for the Highly Stereoselective Hydrosilylation of Alkynes and Alkenes. *Chem. Eur.*
19
20 *J.* **2015**, *21*, 17073–17078. (b) Blug, M.; Le Goff, X.-F.; Mézailles, N.; Le Floch, P. A 14-VE
21
22
23 Platinum(0) Phosphabarrelene Complex in the Hydrosilylation of Alkynes. *Organometallics*
24
25 **2009**, *28*, 2360–2362. (c) Berthon-Gelloz, G.; Schumers, J.-M.; De Bo, G.; Markó, I. E. Highly
26
27 β -(E)-Selective Hydrosilylation of Terminal and Internal Alkynes Catalyzed by a (IPr)Pt(diene)
28
29 Complex. *J. Org. Chem.* **2008**, *73*, 4190–4197. (d) De Bo, G.; Berthon-Gelloz, G.; Tinant, B.;
30
31
32 Markó, I. E. Hydrosilylation of Alkynes Mediated by N-Heterocyclic Carbene Platinum(0)
33
34
35 Complexes. *Organometallics* **2006**, *25*, 1881–1890.

36
37
38 (10) (a) Wu, Y.; Karttunen, V. A.; Parker, S.; Genest, A.; Rösch, N. Olefin Hydrosilylation
39
40
41 Catalyzed by a Bis-N-Heterocyclic Carbene Rhodium Complex. A Density Functional Theory
42
43
44 Study. *Organometallics* **2013**, *32*, 2363–2372. (b) Vicent, C.; Viciano, M.; Mas-Marzá, E.;
45
46
47 Sanaú, M.; Peris, E. Electrospray Ionization Mass Spectrometry Studies on the Mechanism
48
49
50 of Hydrosilylation of Terminal Alkynes Using an N-Heterocyclic Carbene Complex of Iridium,
51
52
53 Allow Detection/Characterization of All Reaction Intermediates. *Organometallics* **2006**, *25*,
54
55
56 3713–3720. (c) Sakaki, S.; Sumimoto, M.; Fukuhara, M.; Sugimoto, M.; Fujimoto, H.;
57
58
59 Matsuzaki, S. Why Does the Rhodium-Catalyzed Hydrosilylation of Alkenes Take Place
60

1
2
3
4
5
6 through a Modified Chalk–Harrod Mechanism? A Theoretical Study. *Organometallics* **2002**,
7
8 *21*, 3788–3802. (d) Itami, K.; Mitsudo, K.; Nishino, A.; Yoshida, J. Metal-Catalyzed
9
10 Hydrosilylation of Alkenes and Alkynes Using Dimethyl(pyridyl)silane. *J. Org. Chem.* **2002**,
11
12 *67*, 2645–2652.

13
14
15
16
17 (11) Tanke, R. S.; Crabtree, R. H. Unusual activity and selectivity in alkyne
18
19 hydrosilylation with an iridium catalyst stabilized by an oxygen-donor ligand. *J. Am.*
20
21 *Chem. Soc.* **1990**, *112*, 7984–7989.

22
23
24
25
26 (12) Ojima, I.; Clos, N.; Donovan, R. J.; Ingallina, P. Hydrosilylation of 1-Hexyne
27
28 Catalyzed by Rhodium and Cobalt-Rhodium Mixed-metal Complexes. Mechanism of
29
30 Apparent Trans Addition. *Organometallics* **1990**, *9*, 3127–3133.
31
32
33
34
35
36
37
38

39
40 (13) Lipke, M. C.; Liberman-Martin, A. L.; Tilley, T. D. Electrophilic Activation of Silicon–
41
42 Hydrogen Bonds in Catalytic Hydrosilations. *Angew. Chem. Int. Ed.* **2017**, *56*, 2260–2294.
43
44

45 (14) Iglesias, M.; Fernández-Álvarez, F. J.; Oro, L. A. Non-classical Hydrosilane Mediated
46
47 Reductions Promoted by Transition Metal Complexes. *Coord. Chem. Rev.* **2019**, *386*, 240–266.
48
49

50 (15) Peris, E. Smart N-Heterocyclic Carbene Ligands in Catalysis. *Chem. Rev.* **2018**, *118*,
51
52 9988–10031.
53
54

55 (16) (a) Tyagi, A.; Yadav, S.; Daw, P.; Ravi, C.; Bera, J. K. A Rh(I) Complex with an
56
57 Annulated N-heterocyclic Carbene Ligand for E-selective Alkyne Hydrosilylation. *Polyhedron*
58
59 **2019**, *172*, 167–174. (b) Morales-Cerón, J. P.; Lara, P.; López-Serrano, J.; Santos, L. L.;
60

1
2
3
4
5
6 Salazar, V.; Álvarez, E.; Suárez, A. Rhodium(I) Complexes with Ligands Based on N-
7
8 Heterocyclic Carbene and Hemilabile Pyridine Donors as Highly E Stereoselective Alkyne
9
10 Hydrosilylation Catalysts. *Organometallics* **2017**, *36*, 2460–2469. (c) Mancano, G.; Page, M.
11
12 J.; Bhadbhade, M.; Messerle, B. A. Hemilabile and Bimetallic Coordination in Rh and Ir
13
14 Complexes of NCN Pincer Ligands. *Inorg. Chem.* **2014**, *53*, 10159–10170. (d) Cassani, M. C.;
15
16 Brucka, M. A.; Femoni, C.; Mancinelli, M.; Mazzanti, A.; Mazzoni, R.; Solinas, G. N-
17
18 Heterocyclic Carbene Rhodium(I) Complexes Containing an Axis of Chirality: Dynamics and
19
20 Catalysis. *New J. Chem.* **2014**, *38*, 1768–1779. (e) Busetto, L.; Cassani, M. C.; Femoni, C.;
21
22 Mancinelli, M.; Mazzanti, A.; Mazzoni, R.; Solinas, G. N-Heterocyclic Carbene-Amide
23
24 Rhodium(I) Complexes: Structures, Dynamics, and Catalysis. *Organometallics* **2011**, *30*,
25
26 5258–5272. (f) Jiménez, M. V.; Pérez-Torrente, J. J.; Bartolomé, M. I.; Gierz, V.; Lahoz, F. J.;
27
28 Oro, L. A. Rhodium(I) Complexes with Hemilabile N-Heterocyclic Carbenes: Efficient Alkyne
29
30 Hydrosilylation Catalysts. *Organometallics* **2008**, *27*, 224–234. (g) Zanardi, A.; Peris, E.; Mata,
31
32 J. A. Alkenyl-Functionalized NHC Iridium-Based Catalysts for Hydrosilylation. *New J. Chem.*
33
34 **2008**, *32*, 120–126. (h) Mas-Marzá, E.; Sanaú, M.; Peris, E. Coordination Versatility of
35
36 Pyridine-Functionalized N-Heterocyclic Carbenes: A Detailed Study of the Different
37
38 Activation Procedures. Characterization of New Rh and Ir Compounds and Study of Their
39
40 Catalytic Activity. *Inorg. Chem.* **2005**, *44*, 9961–9967.

41
42
43
44
45
46
47
48 (17) Iglesias, M.; Sanz Miguel, P. J.; Polo, V.; Fernández-Alvarez, F. J.; Pérez-Torrente, J.
49
50 J.; Oro, L. A. An Alternative Mechanistic Paradigm for the β -Z Hydrosilylation of Terminal
51
52 Alkynes: The Role of Acetone as a Silane Shuttle. *Chem. Eur. J.* **2013**, *19*, 17559–17566.

53
54
55
56 (18) Iglesias, M.; Aliaga-Lavrijsen, M.; Sanz Miguel, P. J.; Fernández-Alvarez, F. J.; Pérez-
57
58 Torrente, J. J.; Oro, L. A. Preferential α -Hydrosilylation of Terminal Alkynes by Bis-N-
59
60 Heterocyclic Carbene Rhodium(III) Catalysts. *Adv. Synth. Catal.* **2015**, *357*, 350–354.

1
2
3
4
5
6 (19) Puerta-Oteo, R.; Jiménez, M. V.; Lahoz, F. J.; Modrego, F. J.; Passarelli, V.; Pérez-
7
8 Torrente, J. J. Zwitterionic Rhodium and Iridium Complexes Based on a Carboxylate Bridge-
9
10 Functionalized Bis-N-heterocyclic Carbene Ligand: Synthesis, Structure, Dynamic Behavior,
11
12 and Reactivity. *Inorg. Chem.* **2018**, *57*, 5526–5543.

13
14
15 (20) Puerta-Oteo, R.; Hölscher, M.; Jiménez, M. V.; Leitner, W.; Passarelli, V.; Pérez-
16
17 Torrente, J. J. Experimental and Theoretical Mechanistic Investigation on the Catalytic CO₂
18
19 Hydrogenation to Formate by a Carboxylate-Functionalized Bis(N-heterocyclic carbene)
20
21 Zwitterionic Iridium(I) Compound. *Organometallics* **2018**, *37*, 684–696.

22
23
24 (21) Puerta-Oteo, R.; Jiménez, M. V.; Pérez-Torrente, J. J. Molecular Water Oxidation
25
26 Catalysis by Zwitterionic Carboxylate Bridge-Functionalized bis-NHC Iridium Complexes.
27
28 *Catal. Sci. Technol.* **2019**, *9*, 1437–1450.

29
30
31 (22) Ojeda-Amador, A. I.; Munarriz, J.; Alamán-Valtierra, P.; Polo, V.; Puerta-Oteo, R.;
32
33 Jiménez, M. V.; Fernández-Alvarez, F. J.; Pérez-Torrente, J. J. Mechanistic Insights on the
34
35 Functionalization of CO₂ with Amines and Hydrosilanes Catalyzed by a Zwitterionic Iridium
36
37 Carboxylate-Functionalized Bis-NHC Catalyst. *ChemCatChem* **2019**, *11*, 5524–5535.

38
39
40 (23) Breit, B.; Gellrich, U.; Li, T.; Lynam, J. M.; Milner, L. M.; Pridmore, N.; Slattery, J.
41
42 M.; Whitwood, C. Mechanistic Insight into the Ruthenium-Catalysed Anti-Markovnikov
43
44 Hydration of Alkynes Using a Self-Assembled Complex: A Crucial Role for Ligand-Assisted
45
46 Proton Shuttle Processes. *Dalton Trans.* **2014**, *43*, 11277–11285.

47
48
49 (24) (a) Jiménez, M. V.; Pérez-Torrente, J. J.; Bartolomé, M. I.; Vispe, E.; Lahoz, F. J.; Oro,
50
51 L. A Cationic Rhodium Complexes with Hemilabile Phosphine Ligands as Polymerization
52
53 Catalyst for High Molecular Weight Stereoregular Poly(phenylacetylene). *Macromolecules*
54
55 **2009**, *42*, 8146–8156. (b) Furlani, A.; Napoletano, C.; Russo, M. V.; Camus, A.; Marsich, N.
56
57
58
59
60

1
2
3
4
5
6 J. The Influence of the Ligands on the Catalytic Activity of a Series of Rh^I Complexes in
7
8 Reactions with Phenylacetylene: Synthesis of Stereoregular Poly(phenyl)acetylene. *Polym.*
9
10 *Sci., Part A: Polym. Chem.* **1989**, *27*, 75–86. (c) Furlani, A.; Napoletano, C.; Russo, M. V.;
11
12 Feast, W. J. Stereoregular Polyphenylacetylene. *Polym. Bull.* **1986**, *16*, 311–317.
13
14

15
16 (25) (a) Xu, C.; Huang, B.; Yan, T.; Cai, M. A Recyclable and Reusable K₂PtCl₄/Xphos-
17
18 SO₃Na/PEG-400/H₂O System for Highly Regio- and Stereoselective Hydrosilylation of
19
20 Terminal Alkynes. *Green Chem.* **2018**, *20*, 391–397. (b) Silbestri, G. F.; Flores, J. C.; de Jesús,
21
22 E. Water-Soluble N-Heterocyclic Carbene Platinum(0) Complexes: Recyclable Catalysts for
23
24 the Hydrosilylation of Alkynes in Water at Room Temperature. *Organometallics* **2012**, *31*,
25
26 3355–3360. (c) Wu, W.; Li, C.-J. A Highly Regio- and Stereoselective Transition Metal-
27
28 catalyzed Hydrosilylation of Terminal Alkynes under Ambient Conditions of Air, Water, and
29
30 Room Temperature. *Chem. Commun.* **2003**, 1668–1669.
31
32
33

34
35 (26) Xuan, Q.-Q.; Ren, C.-Li.; Liu, L.; Wang, D.; Li, C.-J. Copper(II)-catalyzed highly regio-
36
37 and stereo-selective hydrosilylation of unactivated internal alkynes with silylborate in water.
38
39 *Org. Biomol. Chem.* **2015**, *13*, 5871–5874.
40
41

42 (27) (a) Aliaga-Lavrijsen, M.; Iglesias, M.; Cebollada, A.; Garcés, K.; García, N.; Sanz
43
44 Miguel, P. J.; Fernández-Alvarez, F. J.; Pérez-Torrente, J. J.; Oro, L. A. Hydrolysis and
45
46 Methanolysis of Silanes Catalyzed by Iridium(III) Bis-N-Heterocyclic Carbene Complexes:
47
48 Influence of the Wingtip Groups. *Organometallics* **2015**, *34*, 2378–2385. (b) Yu, M.; Jing, H.;
49
50 Liu, X.; Fu, X. Visible-Light-Promoted Generation of Hydrogen from the Hydrolysis of Silanes
51
52 Catalyzed by Rhodium(III) Porphyrins. *Organometallics* **2015**, *34*, 5754–5758. (c) Garcés, K.;
53
54 Fernández-Alvarez, F. J.; Polo, V.; Lalrempuia, R.; Pérez-Torrente, J. J.; Oro, L. A.
55
56 Iridium-Catalyzed Hydrogen Production from Hydrosilanes and Water. *ChemCatChem* **2014**,
57
58 *6*, 1691–1697.
59
60

1
2
3
4
5
6 (28) (a) Poyatos, M.; Mas-Marzá, E.; Mata, J. A.; Sanaú, M.; Peris, E. Synthesis, Reactivity,
7
8 Crystal Structures and Catalytic Activity of New Chelating Bisimidazolium-Carbene
9
10 Complexes of Rh. *Eur. J. Inorg. Chem.* **2003**, 1215–1221. (b) Doyle, M. P.; High, K. G.;
11
12 Nesloney, C. L.; Clayton, T. W., Jr.; Lin, J. Rhodium(II) Perfluorobutyrate Catalyzed
13
14 Hydrosilylation of 1-Alkynes. Trans Addition and Rearrangement to Allylsilanes.
15
16 *Organometallics* **1991**, *10*, 1225-1226.

17
18
19
20 (29) Berben, L. A.; de Bruin, B.; Heyduk, A. F. Non-innocent Ligands. *Chem. Commun.*
21
22 **2015**, *51*, 1553–1554.

23
24
25 (30) Chalk, A. J.; Harrod, J. F. Homogeneous Catalysis. II. The Mechanism of the
26
27 Hydrosilation of Olefins Catalyzed by Group VIII Metal Complexes. *J. Am. Chem. Soc.* **1965**,
28
29 *87*, 16– 21.

30
31
32 (31) Harrod, J. F.; Chalk, A. J., in *Organic Synthesis via Metal Carbonyls*, Vol. 2 (Eds.: I.
33
34 Wender, P. Pino), Wiley, New York, **1977**, p. 673.

35
36
37 (32) Hallam, B. F.; Pauson, P. L. Ferrocene Derivatives. Part III. Cyclopentadienyl iron
38
39 Carbonyls. *J. Chem. Soc.* **1956**, *0*, 3030–3037.

40
41
42 (33) Pitman, C. L.; Finster, O. N. L.; Miller, A. J. M. Cyclopentadiene-Mediated Hydride
43
44 Transfer from Rhodium Complexes. *Chem. Commun.* **2016**, *52*, 9105–9108.

45
46
47 (34) Ji, X.; Yang, D.; Tong, P.; Li, J.; Wang, B.; Qu, J. C-H Activation of Cp* Ligand
48
49 Coordinated to Ruthenium Center: Synthesis and Reactivity of a Thiolate-Bridged Diruthenium
50
51 Complex Featuring Fulvene-like Cp* Ligand. *Organometallics* **2017**, *36*, 1515–1521.

1
2
3
4
5
6 (35) Julián, A.; Guzmán, J.; Jaseer, E. A.; Fernández-Alvarez, F. J.; Royo, R.; García-
7
8 Orduña, P.; Lahoz, F. J.; Oro, L. A. Mechanistic Insights on the Reduction of CO₂ to
9
10 Silylformates Catalyzed by Ir-NSiN species. *Chem. Eur. J.* **2017**, *23*, 11898–11907.
11

12
13 (36) Vásquez-Céspedes, S.; Wang, X.; Glorius, F. Plausible Rh(V) Intermediates in Catalytic
14
15 C–H Activation Reactions. *ACS Catal.* **2018**, *8*, 242–257.
16

17
18 (37) Gabelica, V.; Kresge, A. J. Protonation of Trimethylsilyl-Substituted Carbon–Carbon
19
20 Multiple Bonds in Aliphatic Systems. Conformational Dependence of the β-Silyl Stabilization
21
22 of Carbocations. *J. Am. Chem. Soc.* **1996**, *118*, 3838–3841.
23

24
25 (38) Kozuch, S.; Shaik, S. How to Conceptualize Catalytic Cycles? The Energetic Span
26
27 Model. *Acc. Chem. Res.* **2011**, *44*, 101–110.
28

29
30 (39) (a) Liu, X.-F.; Qiao, C.; Li, X.-Y.; He, L.-N. Carboxylate-promoted reductive
31
32 functionalization of CO₂ with amine and hydrosilane under mild conditions. *Green Chem.*
33
34 **2017**, *19*, 1726–1731. (b) Bleith, T.; Gade, L. H. Mechanism of the Iron(II)-Catalyzed
35
36 Hydrosilylation of Ketones: Activation of Iron Carboxylate Precatalysts and Reaction Pathways
37
38 of the Active Catalyst. *J. Am. Chem. Soc.* **2016**, *138*, 4972–4983. (c) Riduan, S. N.; Zhang, Y.;
39
40 Ying, J. Y. Conversion of carbon dioxide into methanol with silanes over N-heterocyclic
41
42 carbene catalysts. *Angew. Chem. Int. Ed.* **2009**, *48*, 3322–3325.
43
44
45

46
47 (40) Chauvie, P.; Thuéry, P.; Cantat, T. Silyl Formates as Surrogates of Hydrosilanes and
48
49 Their Application in the Transfer Hydrosilylation of Aldehydes. *Angew. Chem. Int. Ed.* **2016**,
50
51 *55*, 14096–14100.
52
53

54
55 (41) O’Hair, R. A. J. The 3D Quadrupole Ion Trap Mass Spectrometer as a Complete
56
57 Chemical Laboratory for Fundamental Gas-Phase Studies of Metal Mediated Chemistry. *Chem.*
58
59 *Commun.* **2006**, 1469–1481
60

1
2
3
4
5
6 (42) Bew, S. P.; Hiatt-Gipson, G. D.; Lovell, J. A.; Poullain, C. Mild Reaction Conditions
7 for the Terminal Deuteration of Alkynes. *Org. Lett.* **2012**, *14*, 456–459.

10
11 (43) Zhong, W.; Fei, Z.; Scopelliti, R.; Dyson, P. J. Alcohol-Induced C–N Bond Cleavage
12 of Cyclometalated N-Heterocyclic Carbene Ligands with a Methylene-Linked Pendant
13 Imidazolium Ring. *Chem. Eur. J.* **2016**, *22*, 12138–12144.

16
17 (44) Vogt, M.; Pons, V.; Heinekey, D. M. Synthesis and Characterization of a Dicationic
18 Dihydrogen Complex of Iridium with a Bis-carbene Ligand Set. *Organometallics* **2005**, *24*,
19 1832–1836.

22
23 (45) Derivatives from *n*-HexC≡CH: (a) Nakamura, S.; Uchiyama, M.; Ohwada, T.
24 Chemoselective Silylzincation of Functionalized Terminal Alkynes Using Dianion-Type
25 Zincate (SiBNOL-Zn-ate): Regiocontrolled Synthesis of Vinylsilanes. *J. Am. Chem. Soc.* **2004**,
26 *126*, 11146–11147. Derivatives from *t*-BuC≡CH: (b) Andavan, G. T. S.; Bauer, E. B.; Letko,
27 C. S.; Hollis, T. K.; Tham, F. S. Synthesis and Characterization of a Free Phenylene bis(N-
28 heterocyclic carbene) and its di-Rh Complex: Catalytic Activity of the di-Rh and CCC-NHC
29 Rh Pincer Complexes in Intermolecular Hydrosilylation of Alkynes. *J. Organomet. Chem.*
30 **2005**, *690*, 5938–5947. Derivatives from Et₃SiC≡CH: (c) Sudo, T.; Asao, N.; Gevorgyan, V.;
31 Yamamoto, Y. Lewis Acid Catalyzed Highly Regio- and Stereocontrolled Trans-
32 Hydrosilylation of Alkynes and Allenes. *J. Org. Chem.* **1999**, *64*, 2494–2499. Derivatives from
33 PhC≡CH and 4-CH₃-C₆H₄C≡CH: (d) Katayama, H.; Taniguchi, K.; Kobayashi, M.; Sagawa,
34 T.; Minami, T.; Ozawa, F. J. Ruthenium-Catalyzed Hydrosilylation of Terminal Alkynes:
35 Stereodivergent Synthesis of (*E*)- and (*Z*)-Alkenylsilanes. *J. Organomet. Chem.* **2002**, *645*,
36 192–200. Derivatives from 4-MeO-C₆H₄C≡CH: (e) Hamze, A.; Provot, O.; Brion, J.-D.; Alami,
37 M. Xphos Ligand and Platinum Catalysts: A Versatile Catalyst for the Synthesis of
38
39
40
41
42
43
44
45
46
47
48
49
50
51
52
53
54
55
56
57
58
59
60

1
2
3
4
5
6 Functionalized β -(E)-vinylsilanes from Terminal Alkynes. *J. Organomet. Chem.* **2008**, *693*,
7 2789–2797. Derivatives from 4-CF₃-C₆H₄C \equiv CH: (f) Hamze, A.; Provot, O.; Brion, J.-D.;
8 Alami, M. Regiochemical Aspects of the Platinum Oxide Catalyzed Hydrosilylation of
9 Alkynes. *Synthesis* **2007**, 2025–2036. Derivatives from t-Bu-C₆H₅-C \equiv CH: (g) Visible light
10 Accelerated Hydrosilylation of Alkynes Using Platinum-[acyclic diaminocarbene]
11 Photocatalysts. Gee, J. C.; Fuller, B. A.; Lockett, H.-M.; Sedghi, G.; Robertson, C. M.;
12 Luzyanin, K. V. *Chem. Commun.* **2018**, *54*, 9450–9453.

23 (46) Yogesh, R. J., Toyoshi, S., An Efficient Method for the Synthesis of Symmetrical
24 Disiloxanes from Alkoxysilanes Using Meerwein's Reagent. *Synlett*, **2012**, *23*, 1633–1638.

28 (47) Frisch, M. J.; Trucks, G. W.; Schlegel, H. B.; Scuseria, G. E.; Robb, M. A.; Cheeseman,
29 J. R.; Scalmani, G.; Barone, V.; Mennucci, B.; Petersson, G. A.; Nakatsuji, H.; Caricato, M.;
30 Li, X.; Hratchian, H. P.; Izmaylov, A. F.; Bloino, J.; Zheng, G.; Sonnenberg, J. L.; Hada, M.;
31 Ehara, M.; Toyota, K.; Fukuda, R.; Hasegawa, J.; Ishida, M.; Nakajima, T.; Honda, Y.; Kitao,
32 O.; Nakai, H.; Vreven, T.; Montgomery Jr. J. A.; Peralta, J. E.; Ogliaro, F.; Bearpark, M.; Heyd,
33 J. J.; Brothers, E.; Kudin, K. N.; Staroverov, V. N.; Kobayashi, R.; Normand, J.; Raghavachari,
34 K.; Rendell, A.; Burant, J. C.; Iyengar, S. S.; Tomasi, J.; Cossi, M.; Rega, N.; Millam, J. M.;
35 Klene, M.; Knox, J. E.; Cross, J. B.; Bakken, V.; Adamo, C.; Jaramillo, J.; Gomperts, R.;
36 Stratmann, R. E.; Yazyev, O.; Austin, A. J.; Cammi, R.; Pomelli, C.; Ochterski, J. W.; Martin,
37 R. L.; Morokuma, K.; Zakrzewski, V. G.; Voth, G. A.; Salvador, P.; Dannenberg, J. J.;
38 Dapprich, S.; Daniels, A. D.; Farkas, Ö.; Foresman, J. B.; Ortiz, J. V.; Cioslowski, J.; Fox, D. J.
39 Gaussian 09, revision D.01; Gaussian, Inc.; Wallingford CT, 2009.

56 (48) Becke, A. D. A New Mixing of Hartree-Fock and Local Density-Functional Theories.
57 *J. Chem. Phys.* **1993**, *98*, 1372–1377.

1
2
3
4
5
6 (49) (a) Grimme, S.; Antony, J.; Ehrlich, S.; Krieg, H. A Consistent and Accurate Ab Initio
7
8 Parametrization of Density Functional Dispersion Correction (DFT-D) for the 94 Elements H-
9
10 Pu. *J. Chem. Phys.* **2010**, *132*, 154104. (b) Johnson, E. R.; Becke, A. D. A Post-Hartree–Fock
11
12 Model of Intermolecular Interactions. *J. Chem. Phys.* **2005**, *123*, 024101.
13
14

15
16 (50) Weigend, F.; Ahlrichs, R. Balanced Basis Sets of Split Valence, Triple Zeta Valence
17
18 and Quadruple Zeta Valence Quality for H to Rn: Design and Assessment of Accuracy. *Phys.*
19
20 *Chem. Chem. Phys.* **2005**, *7*, 3297–3305.
21
22

23
24 (51) Scalmani, G.; Frisch, M. J. Continuous Surface Charge Polarizable Continuum Models
25
26 of Solvation. I. General Formalism. *J. Chem. Phys.* **2010**, *132*, 114110.
27
28

29
30 (52) Tanaka, R.; Yamashita, M.; Chung, L. W.; Morokuma, K.; Nozaki, K. Mechanistic
31
32 Studies on the Reversible Hydrogenation of Carbon Dioxide Catalyzed by an Ir-PNP Complex.
33
34 *Organometallics* **2011**, *30*, 6742–6750.
35
36
37
38
39
40
41
42
43
44
45
46
47
48
49
50
51
52
53
54
55
56
57
58
59
60

Table of Contents Graphic

